From Polygons to Ultradiscrete Painlevé Equations

Christopher Michael ORMEROD † *and Yasuhiko YAMADA* ‡

† *Department of Mathematics, California Institute of Technology, 1200 E California Blvd, Pasadena, CA, 91125, USA*
E-mail: *cormerod@caltech.edu*

‡ *Department of Mathematics, Kobe University, Rokko, 657–8501, Japan*
E-mail: *yamaday@math.kobe-u.ac.jp*

Received January 29, 2015, in final form July 10, 2015; Published online July 23, 2015
http://dx.doi.org/10.3842/SIGMA.2015.056

arXiv:1408.5643v2 [nlin.SI] 23 Jul 2015

Abstract. The rays of tropical genus one curves are constrained in a way that defines a bounded polygon. When we relax this constraint, the resulting curves do not close, giving rise to a system of spiraling polygons. The piecewise linear transformations that preserve the forms of those rays form tropical rational presentations of groups of affine Weyl type. We present a selection of spiraling polygons with three to eleven sides whose groups of piecewise linear transformations coincide with the Bäcklund transformations and the evolution equations for the ultradiscrete Painlevé equations.

Key words: ultradiscrete; tropical; Painlevé; QRT; Cremona

2010 Mathematics Subject Classification: 14T05; 14H70; 39A13

1 Introduction

A significant contribution to our understanding of the Painlevé equations, both discrete and continuous, has been their characterization in terms of their rational surfaces of initial conditions [33, 47]. These works related the symmetries of the Painlevé equations to Cremona isometries of rational surfaces [24, 27, 28], which are groups of affine Weyl type [6, 7, 17]. This provided a geometric setting for many previous studies that were based purely on the symmetries of the Painlevé equations [19, 20, 31]. In the autonomous limit, the Painlevé equations degenerate to elliptic equations or QRT maps [40, 41] and their associated surfaces of initial conditions are rational elliptic surfaces [8, 53].

Given a subtraction free discrete Painlevé equation, one may obtain an ultradiscrete Painlevé equation by applying the ultradiscretization procedure [52]. The ultradiscretization procedure famously related integrable difference equations with integrable cellular automata [49, 51, 52], hence, the process is thought to preserve integrability [21, 43]. The ultradiscrete Painlevé equations are second order non-linear difference equations defined over the max-plus semifield that are integrable in the sense that they possess many of same properties of the continuous and discrete Painlevé equations that are associated with integrability, albeit, in some tropical form. These properties include tropical Lax representations [15, 35] and tropical singularity confinement [14, 36]. They also admit symmetry groups of affine Weyl type [18, 19] and special solutions of rational and hypergeometric type [26, 34, 50]. The ultradiscrete QRT maps may also be obtained as autonomous limits of the ultradiscrete Painlevé equations [29, 39].

The ultradiscrete QRT maps preserve a pencil of curves arising as the level sets of tropical biquadratic functions [29, 39]. Since every non-degenerate level set of a tropical biquadratic function is a tropical genus one curve, one may say that the ultradiscrete QRT maps can be lifted to automorphisms of tropical elliptic surfaces. Given the geometric interpretation of tropical singularity confinement [36], the positions of the rays in any pencil of tropical genus one curves play the same role as the positions of the base points in a pencil of genus one curves. In

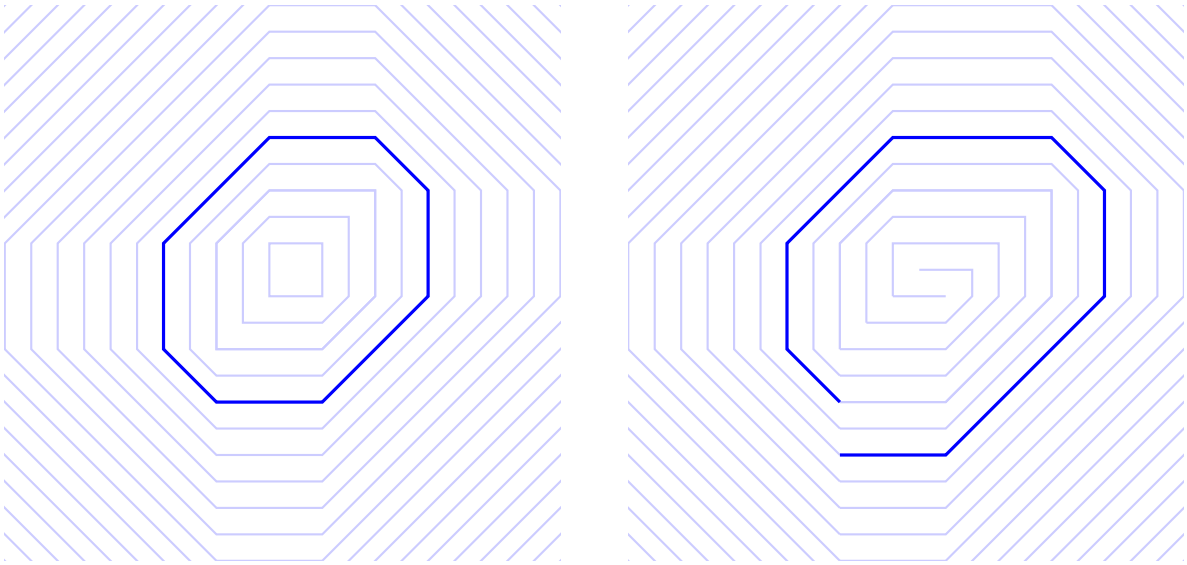


Figure 1. A fibration of closed tropical curves (left) corresponds to ultradiscrete QRT maps. Breaking this closure condition results in spiraling polygons (right), which corresponds to ultradiscrete Painlevé equations.

this way, there is an analogous constraint on the positions of the rays of any pencil of tropical genus one curves, which when removed, results in curves that are no longer closed. We refer to the resulting set of piecewise linear curves as spiraling polygons, which are depicted in Fig. 1. This situation mimics the generalization of elliptic surfaces to surfaces of initial conditions for discrete Painlevé equations.

This article is concerned with groups of piecewise linear transformations of the plane which preserve the forms of the spiraling polygons. We specify a selection spiraling polygons with between three and eleven sides whose groups of transformations form representations of affine Weyl groups with types that coincide with those of the Bäcklund transformations for the multiplicative Painlevé equations [47]. The piecewise linear transformations corresponding to translations in the affine Weyl group are shown to be ultradiscrete Painlevé equations. A list of the correspondences between polygons, symmetry groups and ultradiscrete Painlevé equations, along with where these systems first appeared, is provided in Table 1. This work provides a geometric interpretation for the group of Bäcklund transformations of the ultradiscrete QRT maps and ultradiscrete Painlevé equations.

Our construction replicates the ultradiscretization of known subtraction-free affine Weyl representations in the unpublished work of Kajiwara et al. [18], however, our derivation does not use or require the ultradiscretization procedure. Finding generators for the representations is reduced to combinatorial properties of the underlying polygons. By considering genus one tropical plane cubic, quartic and sextic curves, we treat polygons with up to eleven sides. We mention that the case of octagons arising as level sets of tropical biquadratic functions also appeared in this context in the work of Rojas [46], Nobe [29] and Scully [48], as do a very small collection of the symmetries we list in [46].

We set out this paper as follows: we first briefly review a geometric setting for QRT maps and the discrete Painlevé equations in Section 2, then we review the ultradiscretization procedure with some relevant tools from tropical geometry in Section 3. A description of the canonical classes of transformations that preserve given spiral structures is presented in Section 4, which we use in Section 5 to give explicit presentations of the piecewise linear transformations that may be used to construct the ultradiscrete Painlevé equations. We have a brief discussion of the difficulties in extending this to polygons with greater than eleven sides in Section 6.

Table 1. A labelling of the various polygons and the affine Weyl groups of symmetries they possess. The references refer to the first known appearence of the ultradiscrete Painlevé equation in the literature.

Sides	Polygon	Affine Weyl group	Painlevé equation
3	Triangle	$A_0^{(1)}$	
4	Quadrilateral	$A_1^{(1)}$, $A_1^{(1)}+D_8$	u-P$_{\rm I}$, u-P$'_{\rm I}$ [43]
5	Pentagon	$(A_1+A_1)^{(1)}$	u-P$_{\rm II}$ [43]
6	Hexagon	$(A_2+A_1)^{(1)}$	u-P$_{\rm III}$/ u-P$_{\rm IV}$ [19]
7	Heptagon	$A_4^{(1)}$	u-P$_{\rm V}$ [43]
8	Octagon	$D_5^{(1)}$	u-P$_{\rm VI}$ [43]
9	Enneagon	$E_6^{(1)}$	u-P$\big(A_2^{(1)}\big)$ [18]
10	Decagon	$E_7^{(1)}$	u-P$\big(A_1^{(1)}\big)$ [18]
11	Undecagon	$E_8^{(1)}$	u-P$\big(A_0^{(1)*}\big)$ [18]

2 The geometry of QRT maps and discrete Painlevé equations

The QRT maps are integrable second order autonomous difference equations [40, 41]. They are Lax integrable, measure preserving and possess the singularity confinement property. The QRT maps may broadly be considered discrete analogue of elliptic equations [53]. To construct a QRT map, one takes two linearly independent biquadratics, $h_0(x,y)$ and $h_1(x,y)$, and a generic point, $p=(x,y)$, to which we associate an element, $z=[z_0:z_1]\in\mathbb{P}_1$, by the relation

$$z_0h_0(x,y)+z_1h_1(x,y)=0. \tag{2.1}$$

That is to say that $h_0(x,y)$ and $h_1(x,y)$ define a pencil of biquadratic curves. If we let $h(x,y)=h_0(x,y)/h_1(x,y)$, then the QRT map, $\phi\colon(x,y)\to(\tilde{x},\tilde{y})$, is defined by the condition that $\tilde{x}$ and $\tilde{y}$ are related to x and y by

$$h(x,y)=h(x,\tilde{y}), \tag{2.2a}$$
$$h(x,\tilde{y})=h(\tilde{x},\tilde{y}), \tag{2.2b}$$

where the trivial solutions, $x=\tilde{x}$ and $y=\tilde{y}$, are discarded [40, 41]. In this way, the map is an endomorphism of the curve defined by (2.1) for each value of z.

If we take a point in the intersection of the curves $h_0(x,y)=0$ and $h_1(x,y)=0$, then z_0 and z_1 may be chosen arbitrarily, hence, an entire pencil of curves intersect at these points. These points are called base-points and the number of base points for any pencil of biquadratics is 8, counting multiplicities. A case in which there are eight distinct base points in $\mathbb{R}^2$ is depicted in Fig. 2. By blowing up these base points, possibly multiple times in the case of higher multiplicities, we obtain a surface admitting a fibration by smooth biquadratic curves (i.e., elliptic curves). Lifting the QRT map to this surface gives an automorphism of an elliptic surface [8, 53].

A classic example is the QRT map defined by the invariant

$$h(x,y)=\frac{y}{a_3}+\frac{y}{a_4}+\frac{(a_1+a_2)b_1b_2}{ya_1a_2}+\frac{(y+b_1)(y+b_2)}{xy}+\frac{x(y+b_3)(y+b_4)}{ya_3a_4}, \tag{2.3}$$

where we require the condition

$$a_1a_2b_3b_4=b_1b_2a_3a_4. \tag{2.4}$$

The map, $(x,y)\to(\tilde{x},\tilde{y})$, is specified by relations

$$\tilde{x}x=\frac{a_3a_4(\tilde{y}+b_1)(\tilde{y}+b_2)}{(\tilde{y}+b_3)(\tilde{y}+b_4)}, \tag{2.5a}$$

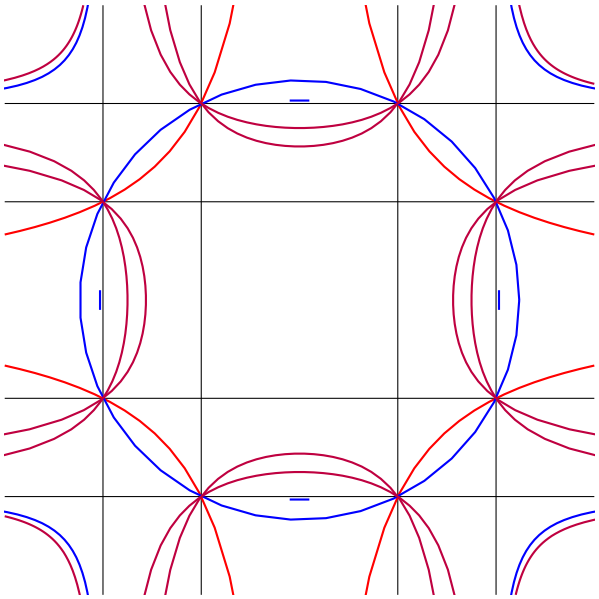


Figure 2. A collection of elements of the pencil of biquadratic curves with eight distinct base-points in $\mathbb{R}^2$.

$$\tilde{y}y = \frac{b_3b_4(x+a_1)(x+a_2)}{(x+a_3)(x+a_4)}. \tag{2.5b}$$

The base points of (2.5) lie on the lines $x, y = 0, \infty$ in $\mathbb{P}^2_1$. The blow-up at these points, with (2.4) as a constraint, is an elliptic surface [8].

The discrete Painlevé equations are integrable second order difference equations that admit the continuous Painlevé equations as a continuum limit [42] and QRT maps in an autonomous limit. The discrete Painlevé equations and QRT maps are integrable by many of the same criteria; Lax integrability [13, 37], vanishing algebraic entropy [2] and singularity confinement [42].

One way to obtain a non-autonomous second order difference equation from a QRT map is by assuming the parameters vary in a manner that preserves the singularity confinement property [42]. Given the autonomous system defined by (2.5), we may deautonomize to the system to obtain the nonlinear q-difference equation

$$\tilde{y}y = \frac{b_3b_4(x+a_1t)(x+a_2t)}{(x+a_3)(x+a_4)}, \tag{2.6a}$$

$$\tilde{x}x = \frac{a_3a_4(\tilde{y}+qb_1t)(\tilde{y}+qb_2t)}{(\tilde{y}+b_3)(\tilde{y}+b_4)}, \tag{2.6b}$$

where $x = x(t)$, $y = y(t)$, $\tilde{x} = x(qt)$ and $\tilde{y} = y(qt)$. If we think of this as a difference equation for $y = y_n$ and $x = x_n$, with independent parameter, n, this is equivalent to n appearing in an exponent as $t = t_0q^n$. The parameter $q \in \mathbb{C} \setminus \{0\}$ is a constant defined by the relation

$$q = \frac{a_1a_2b_3b_4}{b_1b_2a_3a_4}. \tag{2.7}$$

This system was first derived as a connection preserving deformation [13]. While these are often thought of as nonlinear q-difference equations in t, from the viewpoint of symmetries, it is more conducive to think of (2.6) as a map

$$\phi\colon \quad \left(\begin{matrix}a_1, a_2, a_3, a_4\\ b_1, b_2, b_3, b_4\end{matrix}; x, y\right) \to \left(\begin{matrix}qa_1, qa_2, a_3, a_4\\ qb_1, qb_2, b_3, b_4\end{matrix}; \tilde{x}, \tilde{y}\right), \tag{2.8}$$

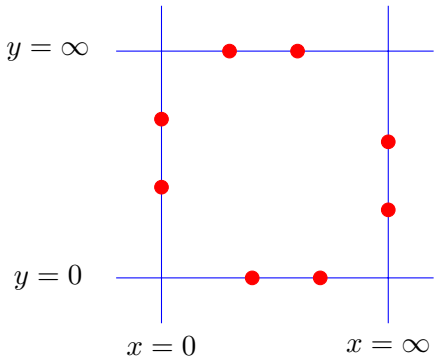


Figure 3. The positions of the blow-up points for (2.5) and (2.6).

where $\tilde{x}$ and $\tilde{y}$ are related by (2.6) and we absorb t into the definitions of a_1, a_2, b_1 and b_2 (equivalent to setting $t = 1$ in (2.6)). When we blow up the eight points, $P = \{p_1, \ldots, p_8\} \subset \mathbb{P}^2_1$, given by

$$\begin{aligned} &p_1 = (-a_1, 0), \qquad p_2 = (-a_2, 0), \qquad p_3 = (-a_3, \infty), \qquad p_4 = (-a_4, \infty),\\ &p_5 = (0, -b_1), \qquad p_6 = (0, -b_2), \qquad p_7 = (\infty, -b_3), \qquad p_8 = (\infty, -b_4), \end{aligned}$$

the resulting surface, X_P, has been called a generalized Halphen surface [47]. Lifting the map defined by (2.6) is not an automorphism of X_P, but rather an isomorphism, $\varphi\colon X_P \to X_{\tilde{P}}$, where $\tilde{P}$ is the set of points defined by the image of (2.8). This map is bijective for the same reasons as for the QRT case. In the autonomous limit as $q = 1$, (2.7) coincides with (2.4), $P = \tilde{P}$ and φ is an automorphism of an elliptic surface that coincides with the lift of (2.5).

In the same way as (2.5), the blow-up points for (2.6) lie on the lines $x, y = 0, \infty$, as shown in Fig. 3. We can identify the affine coordinates, x and y, with projective coordinates, $[x_0 : x_1]$ and $[y_0 : y_1]$, via the relations $x = x_1/x_0$ and $y = y_1/y_0$ in which the points, P, lie on the decomposable curve defined by $x_0x_1y_0y_1 = 0$.

If we were to follow up the construction of the surface, one notices that if we were to interchange the blow-up points, we obtain a surface that is isomorphic. We notice that the blow-up co-ordinates, $(z^1_0 : z^1_1)$ and $(z^3_0 : z^3_1)$, for the points, p_1 and p_3 respectively, satisfy the relations

$$z^1_1(x + a_1) = z^1_0 y, \qquad z^3_1(x + a_3) = \frac{z^3_0}{y},$$

then if we define the transformation $(x, y) \to (\hat{x}, \hat{y})$, by

$$\hat{x} = x, \qquad \hat{y} = y\frac{x + a_3}{x + a_1},$$

then the blow-up co-ordinates in $\hat{x}$ and $\hat{y}$ satisfy the relations

$$z^1_1(\hat{x} + a_3) = z^1_0 \hat{y}, \qquad z^3_1(\hat{x} + a_1) = \frac{z^3_0}{\hat{y}}.$$

This transformation also has a scaling effect on the positions of p_5 and p_6.

$$\left(\begin{matrix} a_1, a_2, a_3, a_4 \\ b_1, b_2, b_3, b_4 \end{matrix}; x, y\right) \to \left(\begin{matrix} a_3, a_2, a_1, a_4 \\ b_1\frac{a_3}{a_1}, b_2\frac{a_3}{a_1}, b_3, b_4 \end{matrix}; \hat{x}, \hat{y}\right). \tag{2.9}$$

Both the constraint, (2.4), and the variable q, defined by (2.7), remain valid on the new surface, hence, the transformation $(x, y) \to (\hat{x}, \hat{y})$ may be lifted to an isomorphism of surfaces.

Let $\sigma_{i,j}$ denote the isomorphism identifying the surfaces in which the blowups at points p_i and p_j are interchanged, then we have a natural set of elements, $w_0 = \sigma_{7,8}$, $w_1 = \sigma_{5,6}$, $w_4 = \sigma_{1,2}$ and $w_5 = \sigma_{3,4}$. We label the transformation from (2.9) by w_3 and the corresponding operation using points p_5 and p_7 by w_2. These transformations and two natural symmetries, ρ_1 and ρ_2, form a representation of an affine Weyl group of type $D_5^{(1)}$ (see [47, Section 2] for more details). Furthermore, as an infinite order isomorphism, both (2.5) and (2.6) may be represented as a product of these involutions as

$$T = \rho_2 \circ w_2 \circ w_0 \circ w_1 \circ w_2 \circ \rho_1 \circ w_3 \circ w_5 \circ w_4 \circ w_3.$$

In many cases, such birational representations were studied independently.

While we have been considering biquadratics over $\mathbb{P}_1^2$, we may extend these arguments to plane curves in $\mathbb{P}_2$ via the birational map, $\pi\colon \mathbb{P}_1^2 \to \mathbb{P}_2$, defined by

$$\pi\colon \ ([x_0 : x_1], [y_0 : y_1]) = [x_0 y_0 : x_1 y_0 : x_0 y_1],$$

which is not defined when $x_0 = y_0 = 0$ (corresponding to (∞, ∞)). The inverse,

$$\pi^{-1}([u_0 : u_1 : u_2]) = ([u_0 : u_1], [u_0 : u_2]),$$

is not defined at $[0 : 0 : 1]$ and $[0 : 1 : 0]$. These maps are isomorphisms when restricted to the copies of $\mathbb{C}^2$ defined by $x_0 = y_0 = 1$ and $u_0 = 1$ respectively (or more precisely, x_0, y_0 and u_0 are not 0). Any biquadratic curve,

$$b(x, y) = \sum b_{i,j} x_0^i x_1^{2-i} y_0^j y_1^{2-j} = 0,$$

going through (∞, ∞) (i.e., $b_{2,2} = 0$) is mapped, via π, to a cubic plane curve

$$c(u) = \sum_{0 \le i,j \le 2, i+j>0} c_{i,j} u_0^{i+j-1} u_1^{2-i} u_2^{2-j},$$

which goes through $[0 : 0 : 1]$ and $[0 : 1 : 0]$. In this way, our two generating biquadratics, h_0 and h_1 from (2.1), map to two cubic planar curves which generally intersect at 9 points (also constrained). In this way, we can naturally pass from a pencil of biquadratics on $\mathbb{P}_1^2$, which is resolved by blowing up eight points to a pencil of cubic plane curves, and a surface obtained by blowing up $\mathbb{P}_2$ at nine points.

In passing from the QRT maps to discrete Painlevé equations via singularity confinement, where the base points are allowed to move, the resulting systems are one of three types of nonautonomous difference equations; h-difference, q-difference or elliptic difference equations. The points can still lie in non-generic positions, but the additional constraint associated with the QRT maps is relaxed. The positions and multiplicities of these nine points determine the symmetries of the surface and of the equation. All the equations admitting ultradiscretization (or tropicalization) are special cases of q-difference equations, where all the parameters are assumed to be positive. The class of surfaces giving rise to q-difference equations was studied by Looijenga [24].

When the nine points are in any non-generic position and appear with different multiplicities, one can not interchange blow-up points in any ad-hoc manner. For example, in the case of (2.5), the points lie on four distinct lines with an intersection form of type $A_3^{(1)}$, and the positions of those points are subject to the constraint (2.4). The type of surface is characterized by this intersection form, and we may only interchange blow-up points in a way that preserves the intersection form. In this way we obtain two root systems, one describing the symmetry group of the equation, the other describing the surface type. A degeneration diagram which lists the surface type and the symmetries of the corresponding q-Painlevé equations is given in Fig. 4.

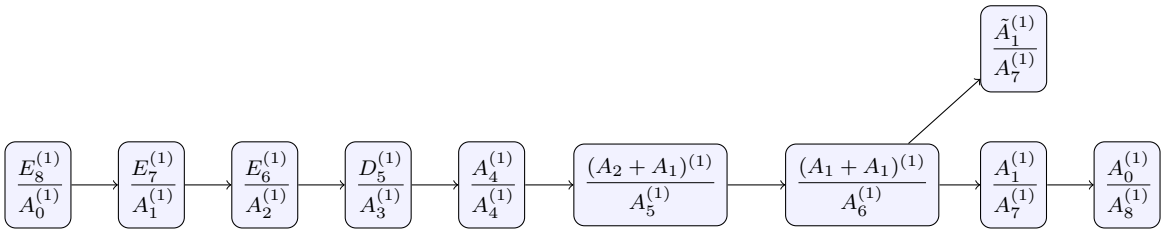


Figure 4. The coalescence diagram for q/u-Painlevé equations. The symmetry of the equation appears on top and the surface type appears below.

By identifying the Picard lattices of isomorphic surfaces, we have an alternative interpretation of these maps and their symmetries [47]. From the theory of rational surfaces (as blow-ups of the minimal surfaces $\Sigma_0 = \mathbb{P}_1^2$ or $\Sigma_1 = \mathbb{P}_2$), we have the isomorphism $\mathrm{Pic}(X) = \mathbb{H}^1(X, \mathcal{O}^*) \cong H_2(X, \mathbb{Z})$, with an endowed intersection form [27, 28]. The interchange of blow-up and blow-down structures [1] preserves this intersection form and leaves the canonical class fixed [24], so we may interpret these as reflections in $\mathrm{Pic}(X)$. This defines a group of Cremona isometries, which are of affine Weyl type. The work of Sakai extended [24] and realized the action of the translational Cremona isometries as discrete Painlevé equations [47].

3 Tropicalization

Tropicalization can be thought of as the pointwise application of a nonarchimedean valuation to geometric structures. Tropicalization sends curves to lines, surfaces to polygons and more generally, smooth structures to piecewise linear ones [3, 45]. In the integrable community a non-analytic limit known as ultradiscretization is used as a way of obtaining new and interesting piecewise linear integrable systems [52]. Relating tropicalization with ultradiscretization gives us a way of understanding the geometry of ultradiscrete systems [36].

Let us first consider the ultradiscretization procedure as it was originally considered in [52]. Given a subtraction free rational function in a number of strictly positive variables, $f(x_1, \ldots, x_n)$, we introduce ultradiscrete variables, $X_1, \ldots, X_n$, related by $x_i = e^{X_i/\epsilon}$. The ultradiscretization of f, denoted F, is obtained by the limit

$$F(X_1, \ldots, X_n) := \lim_{\epsilon \to 0^+} \epsilon \ln f(x_1, \ldots, x_n). \tag{3.1}$$

The subtraction free nature of the function is required so that we need not consider the logarithm of a negative number. Roughly speaking, the ultradiscretization procedure replaces variables and binary operations as follows:

$$x_1 x_2 \to X_1 + X_2, \qquad x_1 + x_2 \to \max(X_1, X_2), \qquad x_1 / x_2 \to X_1 - X_2,$$

where there is no (natural) replacement of subtraction.

Given a difference equation, such as (2.6), we may apply the ultradiscretization procedure to obtain a system known as u-P$_{\mathrm{VI}}$ [43], given by

$$\begin{aligned} X + \tilde{X} &= A_3 + A_4 + \max(Q + T + B_1, \tilde{Y}) + \max(Q + T + B_2, \tilde{Y}) \\ &\quad - \max(B_3, \tilde{Y}) - \max(B_4, \tilde{Y}), \end{aligned} \tag{3.2a}$$

$$\begin{aligned} Y + \tilde{Y} &= B_3 + B_4 + \max(A_1 + T, \tilde{X}) + \max(A_2 + T, X) \\ &\quad - \max(B_3, X) - \max(B_4, X), \end{aligned} \tag{3.2b}$$

where the variable Q is specified by the relation

$$Q = A_1 + A_2 - A_3 - A_4 - B_1 - B_2 + B_3 + B_4.$$

A special case of this system was shown to arise as an ultradiscrete connection preserving deformation [35]. In the same way as (2.6), we may think of this as a map

$$\Phi\colon \quad \begin{pmatrix} A_1, A_2, A_3, A_4 \\ B_1, B_2, B_3, B_4 \end{pmatrix}; X, Y \Bigg) \to \begin{pmatrix} Q + A_1, Q + A_2, A_3, A_4 \\ Q + B_1, Q + B_2, B_3, B_4 \end{pmatrix}; \tilde{X}, \tilde{Y} \Bigg).$$

In the autonomous limit, when we let $Q = 0$, the above ultradiscrete Painlevé equation becomes an ultradiscrete QRT map (i.e., the ultradiscretization of (2.5)), which was introduced in [39] and studied from a tropical geometric viewpoint by Nobe [29]. The ultradiscretization of (2.3) gives the following piecewise linear function

$$\begin{aligned} H(X, Y) = \max\big(&Y - A_3, Y - A_4, B_1 + B_2 \max(-A_1, -A_2) - Y, \\ &\max(Y, B_1) + \max(Y, B_2) - X - Y, \\ &X - Y + \max(Y, B_3) + \max(Y, B_4) - A_3 - A_4\big), \end{aligned} \tag{3.3}$$

which is also an invariant of the ultradiscrete QRT map, i.e., $H(X, Y) = H(\tilde{X}, \tilde{Y})$ [29]. Furthermore, the evolution of the ultradiscrete QRT map defines a linear evolution on the Jacobian of the invariant, hence, the ultradiscrete QRT map may be expressed in terms of the addition law on a tropical elliptic curve [5, 29].

While we may be able to solve (2.2) in a subtraction free manner, given an invariant such as (3.3), the equation $H(X, Y) = H(\tilde{X}, \tilde{Y})$ involves a max on both the left and right, hence, cannot generally be solved within the limited framework of tropical arithmetic. Our approach is different in that we only consider transformations that preserve the structure of the tropical curves of the form $H(X, Y) = H_0$ where H_0 is some constant. Any automorphism of tropical curves of this form can be expressed in terms of compositions of more fundamental operations. We need to consider these curves more carefully, hence, we will briefly review some tropical geometry [45].

The discrete dynamical system, (3.2), is most naturally defined over a tropical semifield [38], more precisely, the max-plus semifield, which is the set $\mathbb{T} = \mathbb{R} \cup \{-\infty\}$, equipped with the binary operations

$$X_1 \oplus X_2 := \max(X_1, X_2), \qquad X_1 \otimes X_2 := X_1 + X_2,$$

which are known as tropical addition and tropical multiplication respectively. The element $-\infty$ plays the role of the tropical additive identity and 0 plays the role of the tropical multiplicative identity [38].

The geometry of objects over the tropical semifields is the subject of tropical geometry [45]. A tropical polynomial, $F \in \mathbb{T}[X_1, \ldots, X_n]$ defines a piecewise linear function from $\mathbb{T}^n \to \mathbb{T}$, given by

$$F(X_1, \ldots, X_n) = \max_j (C_j + A_{j,1} X_1 + \cdots + A_{j,n} X_n), \tag{3.4}$$

where $\{A_{j,i}\}$ is a set of integers and $\{C_j\}$ is a set of elements of $\mathbb{T}$. The tropical variety associated with $F \in \mathbb{T}[X_1, \ldots, X_n]$, denoted $\mathcal{V}(F)$, is defined to be

$$\mathcal{V}(F) = \big\{X = (X_1, \ldots, X_n) \in \mathbb{T}^n \text{ such that } F \text{ is not differentiable at } X\big\},$$

which occurs precisely when one argument of the max-expression becomes dominant over another argument [45].

Another equivalent algebraic characterization of tropical varieties relies on nonarchimedean valuations. Every non-zero algebraic function, $f \in \mathbb{C}(t)$, admits a representation as a Puiseux series,

$$f(t) = c_1 t^{q_1} + c_2 t^{q_2} + \cdots,$$

where $c_1 \neq 0$ and $\{q_i\}$ are rational and ordered such that $q_i < q_{i+1}$. The function, $\nu\colon \mathbb{C}(t) \to \mathbb{T}$, given by

$$\nu(f) = -q_1,$$

is a nonarchimedean valuation. This may be extended to an algebraically and topologically closed field with a valuation ring of $\mathbb{R}$, which we simply denote $\mathbb{K} = \overline{\mathbb{C}(t)}$ [25]. If $I \subset \mathbb{K}[x_1^{\pm 1}, \ldots, x_n^{\pm 1}]$ is an ideal, then we define $V(I) \subset \mathbb{K}^n$ as

$$V(I) = \{(x_1, \ldots, x_n)\colon\ f(x_1, \ldots, x_n) = 0 \text{ for all } f \in I\}.$$

The tropical variety associated with I is the topological closure of the point-wise application of ν to $V(I)$, i.e., $\mathcal{V}(I) = \overline{\nu(V(I))} \subset \mathbb{T}^n$. For every tropical variety $\mathcal{V}(F)$, there exists a function, f, such that $\mathcal{V}(F) = \mathcal{V}(\langle f \rangle)$ where $\langle f \rangle \subset \mathbb{K}[x_1^{\pm 1}, \ldots, x_n^{\pm 1}]$ denotes the ideal generated by f. This means that we may define a tropical variety in terms of either piecewise linear functions or ideals of $\mathbb{K}[x_1^{\pm 1}, \ldots, x_n^{\pm 1}]$. The equivalence of the set of points of non-differentiability and the image of the valuations is outlined in [45]. Each tropical curve is a collection vertices, finite line segments, called edges, and a collection of semi-infinite line segments, called rays.

In the same way as affine n-space may be considered to be embedded in projective space, we may naturally consider $\mathbb{T}^n$ as being embedded in tropical projective space. Define the equivalence relation, $\sim$, on $\mathbb{T}^{n+1}$ so that

$$V \sim U \quad \text{if and only if} \quad V = U + \lambda(1, 1, \ldots, 1),$$

for some λ, then tropical projective n-space is the set

$$\mathbb{TP}_n = \mathbb{T}^{n+1} / \sim .$$

A tropical function of the form (3.4) is said to be homogeneous if there exists a d such that for every j

$$\sum_i A_{j,i} = d.$$

The set of non-differentiable points of a tropically homogeneous polynomial defines a tropical projective variety.

Given a rational function in a number of variables, $f(x_1, \ldots, x_n)$, we can lift the function up to the field of algebraic functions by letting $x_i = t^{X_i}$ for some X_i, then the ultradiscretization procedure is known to coincide with

$$F(X_1, \ldots, X_n) = \nu(f(x_1, \ldots, x_n)), \tag{3.5}$$

for all subtraction free functions [34, 36]. The above extension, given by (3.5), is one of a number of ways to incorporate a version of subtraction into the ultradiscretization procedure [12, 22, 23, 32].

The most immediate consequence from the viewpoint of the geometry is that singularities of a map manifest themselves as points of non-differentiability [3, 36, 45]. This interpretation was

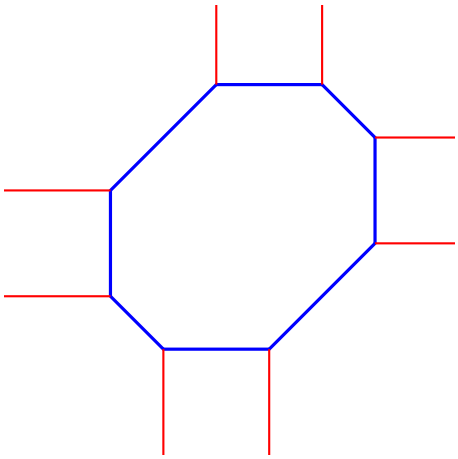


Figure 5. A tropical biquadratic with the rays labeled in red.

also present in the work of Joshi and Lafortune who elucidated what the analogue of singularity confinement should be for tropical integrable difference equations [14].

One of the characteristic features of the QRT map is that the invariant curves all intersect at the base points. From looking at the invariant curves of (2.5), depicted in Fig. 1, this feature is not apparent in the tropical setting. When we consider the extension of the ultradiscretization via (3.5), another way of looking at the invariant is that the level set is a subset of the tropical variety associated the ideal

$$I_{H_0} = \langle h(x,y) - t^{H_0} \rangle,$$

in $\mathbb{K}[x,y]$, which is the set

$$\mathcal{V}(I_{H_0}) := \overline{\nu(V(I_{H_0}))}. \tag{3.6}$$

For each $x = t^X$ where $X \in \mathbb{Q}$, the equation

$$h\big(t^X, y\big) - t^{H_0} = 0,$$

is quadratic in y, and as $\mathbb{K}$ is algebraically closed, we have two algebraic solutions, y_1 and y_2 over $\mathbb{K}$. That is for each X, we obtain values $Y_1 = \nu(y_1)$ and $Y_2 = \nu(y_2)$ in $\mathbb{T}$, which form infinite rays (also called tentacles in [5, 29]). These form points of $\mathcal{V}(I_{H_0})$ that do not appear in the level set of $H(X,Y)$. Notice that each of the rays intersect on the lines at $X = \pm\infty$ and $Y = \pm\infty$, and positions of the rays define where on that line they intersect. The inclusion of the rays to the level sets, as seen in Fig. 5, makes them smooth tropical curves in the sense of [45].

We may extend these tropical biquadratics to $\mathbb{TP}^2_1$ by using homogeneous co-ordinates $X = [X_0 : X_1]$ and $Y = [Y_0 : Y_1]$. The maps π and π^{-1} possess tropical analogues, $\Pi\colon \mathbb{TP}^2_1 \to \mathbb{TP}_2$ and $\Pi^{-1}\colon \mathbb{TP}_2 \to \mathbb{TP}^2_1$, given by

$$\begin{aligned} \Pi\colon &\quad ([X_0, X_1], [Y_0, Y_1]) \to [X_0 + Y_0 : X_1 + Y_0 : X_0 + Y_1], \\ \Pi^{-1}\colon &\quad [U_0 : U_1 : U_2] \to ([U_0 : U_1], [U_0 : U_2]). \end{aligned}$$

These are isomorphisms between the copies of $\mathbb{T}^2$ specified by $X_0 = Y_0 = 0$ and $U_0 = 0$ respectively. The map Π is not defined when $X_0 = Y_0 = -\infty$ and the inverse is not defined at $[-\infty : 0 : -\infty]$ and $[-\infty : -\infty : 0]$. The level set of a tropical biquadratic function

$$H(X,Y) = \max_{i,j=0,1,2} \big(B_{i,j} + iX_0 + (2-i)X_1 + jY_0 + (2-j)Y_1\big),$$

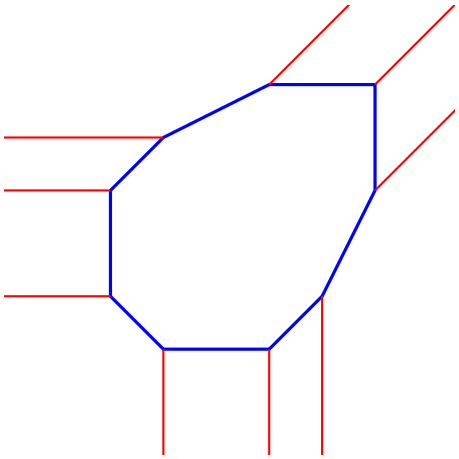


Figure 6. A tropical cubic plane curve with rays labeled in red.

in which $B_{2,2} = -\infty$ maps via Π to a tropical cubic plane curve, specified by the level set of some cubic,

$$H(U) = \max_{0\leq i,j\leq 2,\, i+j>0} \big(C_{i,j} + (i+j-1)U_0 + (2-i)U_1 + (2-j)U_2\big).$$

Since Π maps the rays and edges over $\mathbb{TP}^2_1$ to rays and edges in $\mathbb{TP}_2$, we expect the image of the level set of a biquadratic to be at most an octagon, however, the most general cubic plane curve is an enneagon. If one considers the enneagon as the image of the variety over $\mathbb{K}[x,y,z]$, one recovers nine rays counting multiplicities. The case of nine distinct rays is depicted in Fig. 6. In this way, the information we have on rays in $\mathbb{P}^2_1$ applies equally well to the rays in $\mathbb{TP}_2$.

As the rays define the positions of the vertices of each polygon, they will play an important role in the description of the symmetries. In Figs. 5 and 6, all the rays are asymptotic to one of three forms;

$$L_i\colon\ X - A_i = 0, \qquad L_j\colon\ Y - A_j = 0, \qquad L_k\colon\ Y - X - A_k = 0.$$

Since the rays in Figs. 5 and 6 are part of every variety of the form (3.6), this is equivalent to each variety intersecting in $\mathbb{TP}_2$ at points

$$[A_i : -\infty : 0], \qquad [-\infty : A_j : 0], \qquad [0 : -\infty : A_k],$$

respectively. For the level set to close, there is a constraint on the positions of the rays, which when relaxed gives a spiral diagram. For smooth biquadratics, we obtain spiraling octagons (see Fig. 1). In the smooth cubic case we obtain spiraling enneagons (see Fig. 19). Given a polygon arising as a tropical curve, there are two types of degenerations:

- We may make two parallel rays coincide.
- We may take two rays that are not parallel and merge them.

The latter corresponds to setting a coefficient of $H(X,Y)$ to $-\infty$.

This construction may be generalized to tropical genus one curves of higher degrees, which allows us to consider decagons and undecagons as level sets of tropical quartic and tropical sextic plane curves respectively. In these cases, one finds twelve and thirteen rays, counting multiplicities (when rays coincide). The decagon used will be a tropical quartic with four rays of order one of the form $L_i\colon X - A_i$, four rays of order one of the form $L_j\colon Y - A_j$ and two rays of order two of the form $L_k\colon Y - X - A_k = 0$. This would be the ultradiscretization of a curve

of degree four with eight singularities of order one and two of order two, which gives a genus of one curve by the degree-genus formula,

$$g = \frac{(d-1)(d-2)}{2} - \sum_k \frac{r_k(r_k-1)}{2}, \tag{3.7}$$

where d is the degree of the curve and the r_i is the order of the k-th singularity. In a similar way, our undecagon is a the ultradiscretization of a genus one curve of degree six curve with six rays of order one, two of order three and three of order two. This formula remains valid for tropical varieties [9].

4 Piecewise linear transformations of polygons and spirals

Cremona transformations of the plane, and their subgroups, are a topic of classical and modern interest [6, 10, 17]. The classical result of Noether [30] (see also [10]) states that Cremona transformations are generated by the quadratic transformations, the simplest being the standard Cremona transformation

$$\tau\colon\ [x:y:z] \to [yz:xz:xy],$$

which may be interpreted as the blow-up of the points $[1:0:0]$, $[0:1:0]$ and $[0:0:1]$ combined with a blow-down on the co-ordinate lines given by $xyz=0$. In a similar vein, our aim is to specify a generating set of tropical Cremona transformations from which all the other transformations may be obtained. Our aim is to specify subgroups of these that preserve a given spiral diagram.

To specify any spiral diagram, we begin with a parameterization of the asymptotic form of the rays,

$$\mathcal{X} = \{L_i \text{ where } L_i\colon\ a_iX + b_iY + c_i = 0,\ \text{and } a_i, b_i, c_i \in \mathbb{Z}\}.$$

The shape of the spirals are determined by the invariants obtained in the autonomous limit. We seek a group of transformations that preserve the forms of these rays, more specifically, we seek transformations, σ, such that

1) σ is a bijection of the plane;
2) for every ray, L_j, there is a ray, L_i, such that $\sigma\colon L_i = \tilde{L}_j$, where $\tilde{L}_j$ differs only by some translation.

These may be thought of as tropical Cremona isometries, as these conditions replicate conditions that require the canonical class and intersection form of the surface be fixed.

Since the Cremona isometries are products of the interchange of blow-up and blow-down structures [1], and the positions of these blow-up points are encoded in the positions of the rays, it is sufficient to consider the shearing transformations that create and smooth out polygons whose vertices lie along these rays. Analagously to the results of Noether [10], we propose the following two generators:

$$\iota_A\colon\ (X,Y) \to (X, Y + \max(0, X - A)), \tag{4.1}$$
$$\Xi\colon\ (X,Y) \to (aX + cY, bX + dY), \tag{4.2}$$

where $|ad-bc| = 1$ and $A \in \mathbb{T}$. The action of ι_A can be seen as an analogous to the interchange of blow-ups in the following way: if the vertices of the level sets of a polygon trace out the rays, then ι_A can smooth out all the vertices along a ray asymptotic to, $L\colon X = A$, while

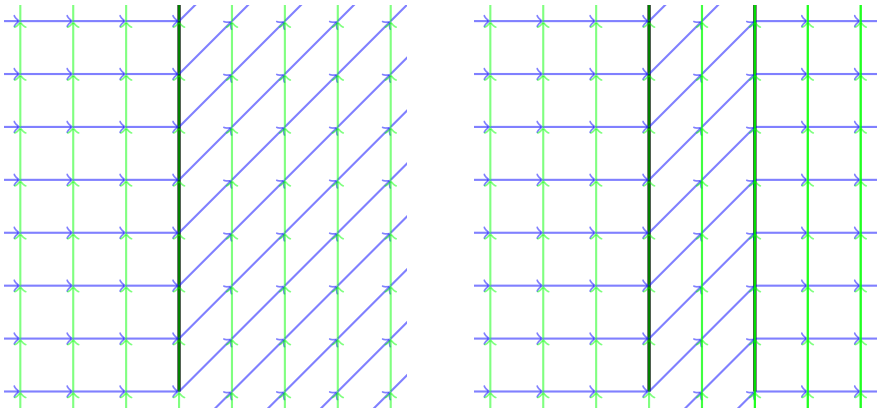


Figure 7. Assuming $B < A$, the effect of ι_B is depicted on the left, and $\sigma = \iota_A^{-1} \circ \iota_B$ on the right.

simultaneously creating a kink along all the level sets along a ray of the same form, but in the opposite direction. This means that if all the rays intersected at a point $P = (A, -\infty)$, the transformed polygon has rays that intersect at (A, ∞), or vise versa.

Let us use ι_A to interchange rays that are of the same form in asymptotically opposite directions. Suppose we have two rays, L_i and L_j, which satisfy

$$L_i\colon\ X - A = 0 \qquad \text{and} \qquad L_j\colon\ X - B = 0,$$

as $Y \to -\infty$ and $Y \to \infty$ respectively. In the simplest case, these rays are order one, in that the change in derivative is just one, in which case the transformation

$$\sigma = \iota_B^{-1} \circ \iota_A\colon\ (X, Y) \to (X, Y + \max(0, X - A) - \max(0, X - B)),$$

has the effect of creating a ray along the line $X - A$ as $Y \to \infty$ and smooting out a set of kinks along L_i, and conservely doing the same for L_j. If we think of the surface as being parameterized by A and B, then this action has the effect of swapping A and B. The overall shape of the resulting polygon does not change by this transformation and the action is an isomorphism of polygons. The action of ι_A and σ on the plane is depicted in Fig. 7 and the action on the level set of the form in Fig. 5 is depicted in Fig. 8.

Let us now consider how to swap rays given by

$$L_i\colon\ X - A = 0, \qquad L_j\colon\ Y - B = 0,$$

as $Y \to -\infty$ and $X \to -\infty$ respectively. To describe this transformation, let us consider the transformation, $\rho\colon \mathbb{T}^2 \to \mathbb{T}^2$, given by

$$\rho\colon\ (X, Y) \to (X - \max(0, Y), X - \max(0, -Y)),$$

whose inverse is given by

$$\rho^{-1}\colon\ (X, Y) \to (\max(X, Y), Y - X).$$

This transformation can be expressed as a composition of transformations of the form (4.1) and (4.2) as

$$\begin{aligned}\rho\colon\ (X, Y) &\xrightarrow{\Xi} (Y, X) \xrightarrow{\iota_0} (Y, X - \max(0, Y)) \xrightarrow{\Xi} (X - \max(0, Y), Y) \\ &\xrightarrow{\Xi} (X - \max(0, Y), Y + X - \max(0, Y)) = (X - \max(0, Y), X - \max(0, -Y)).\end{aligned}$$

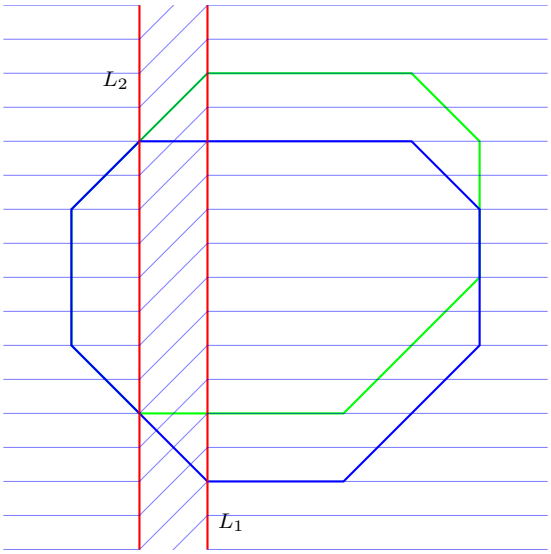


Figure 8. A depiction of action of σ, described above on an octagon with rays L_1 and L_2. The blue octagon is the preimage and the green octagon is the image.

Roughly speaking, this sends every straight line of the form $X - A = 0$ to one that is bent 90 degree along the line $Y = X$. The conjugation of ι_A by ρ, which we label $\eta_A = \rho \circ \iota_A \circ \rho^{-1}$, is given by the expression

$$\eta_A(X, Y) = (X - \max(0, Y - A), Y + \max(A, X, Y) - \max(A, Y)).$$

It should be clear that this has the same effect as ι_A below the line $Y = X$, however, the effect of ι_A around $Y = \infty$ now occurs at $X = -\infty$. We may now state that the transformation swapping L_i and L_j is given by

$$\sigma = \eta_B \circ \eta_A^{-1},$$

whose max-plus expression may be simplified to

$$\begin{aligned}\sigma(X, Y) = \big(&B + X + \max(A, X, Y) - \max(A + B, B + X, A + Y),\\ &A + Y + \max(B, X, Y) - \max(A + B, B + X, A + Y)\big),\end{aligned} \tag{4.3}$$

or equivalently, this is the tropical projective transformation

$$\begin{aligned}\sigma([X : Y : Z]) = \big[&B + X + \max(A + Z, X, Y) : A + Y + \max(B + Z, X, Y) :\\ &Z + \max(A + B + Z, B + X, A + Y)\big].\end{aligned}$$

The effect of η_B is shown in Fig. 9 and the effect on a cubic plane curve with these rays is depicted in Fig. 10.

Lastly, for bookkeeping reasons, we include a set of transformations simply permute the roles of two rays that are of the same type. For example, if we have a tentacle, described by $L_i \colon X - A = 0$ as $Y \to -\infty$ and another, described by $L_j \colon X - B = 0$ as $Y \to -\infty$, then one transformation simply swaps the roles of A and B, which swaps L_i and L_j. In this case, σ acts as the identity map on the plane and as a simple transformation of the parameter space. This transformation can always be applied when there are two rays of the same form.

Each of these transformations is an isomorphism between either a collection of polygons or between some spiral diagrams of the same form. We can now specify that each of the

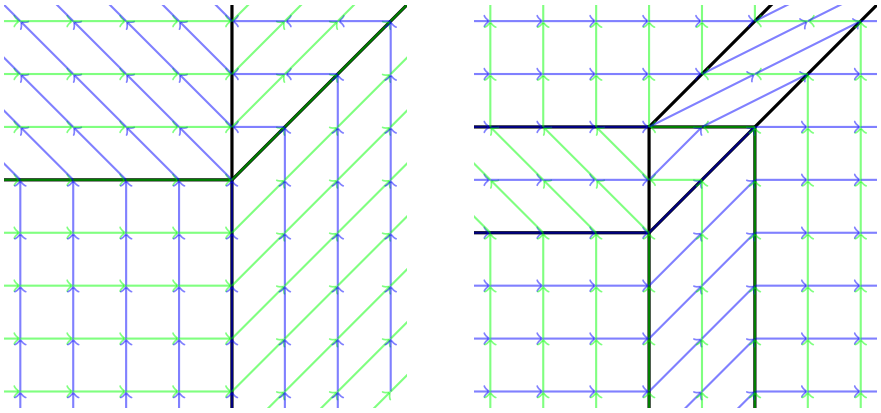


Figure 9. The action of η_B and σ from (4.3) on $\mathbb{TP}_2$.

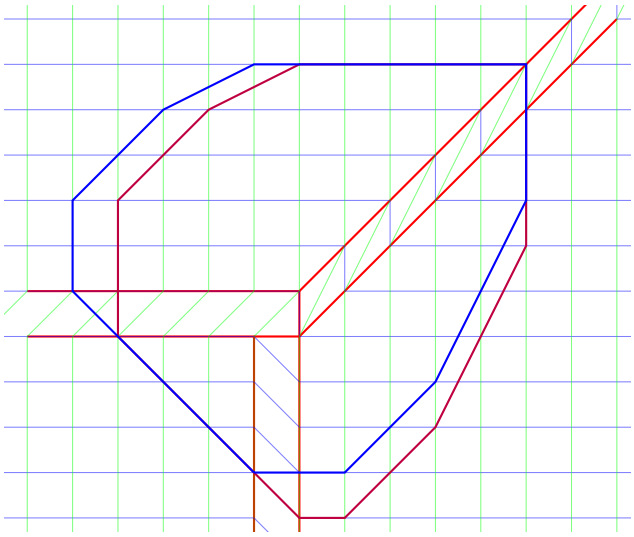


Figure 10. The effect of the σ from (4.3) on a tropical cubic plane curve with rays $L_i\colon X - A = 0$ and $L_j\colon Y - B = 0$.

ultradiscrete QRT maps and ultradiscrete Painlevé equations are infinite order elements of the group of transformations that preserve a pencil of polygons defined by tropical genus one curves or their corresponding spiral diagrams respectively. This means they may be expressed in terms of the simple transformations above. As an example, we consider (2.5) and (2.6). We start by parameterizing the rays as follows:

$$\begin{aligned} &L_1\colon\ X - A_1 = 0, \quad && L_2\colon\ X - A_2 = 0, \quad && L_3\colon\ X - A_3 = 0, \quad && L_4\colon\ X - A_4 = 0,\\ &L_5\colon\ Y - B_1 = 0, \quad && L_6\colon\ Y - B_2 = 0, \quad && L_7\colon\ Y - B_3 = 0, \quad && L_8\colon\ Y - B_4 = 0, \end{aligned}$$

where L_1 and L_2 extend downwords, L_3 and L_4 extend upwards, L_5 and L_6 extend to the left and L_7 and L_8 extend to the right. We now have a group of type $W(D_5^{(1)}) = \langle s_0, \ldots, s_5\rangle$ where

$$\begin{aligned} &s_0 = \sigma_{7,8}, \quad && s_1 = \sigma_{5,6}, \quad && s_2 = \sigma_{5,7},\\ &s_3 = \sigma_{1,3}, \quad && s_4 = \sigma_{1,2}, \quad && s_3 = \sigma_{3,4}, \end{aligned}$$

with two additional symmetries, p_1 and p_2, which are reflections through the line $Y = (B_3 + B_4)/2$ and $X = (A_3 + A_4)/2$ respectively. We can now write the ultradiscrete QRT map and the ultradiscrete Painlevé equation as the composition

$$T = p_2 \circ s_2 \circ s_0 \circ s_1 \circ s_2 \circ s_1 \circ p_1 \circ s_3 \circ s_5 \circ s_4 \circ s_3. \tag{4.4}$$

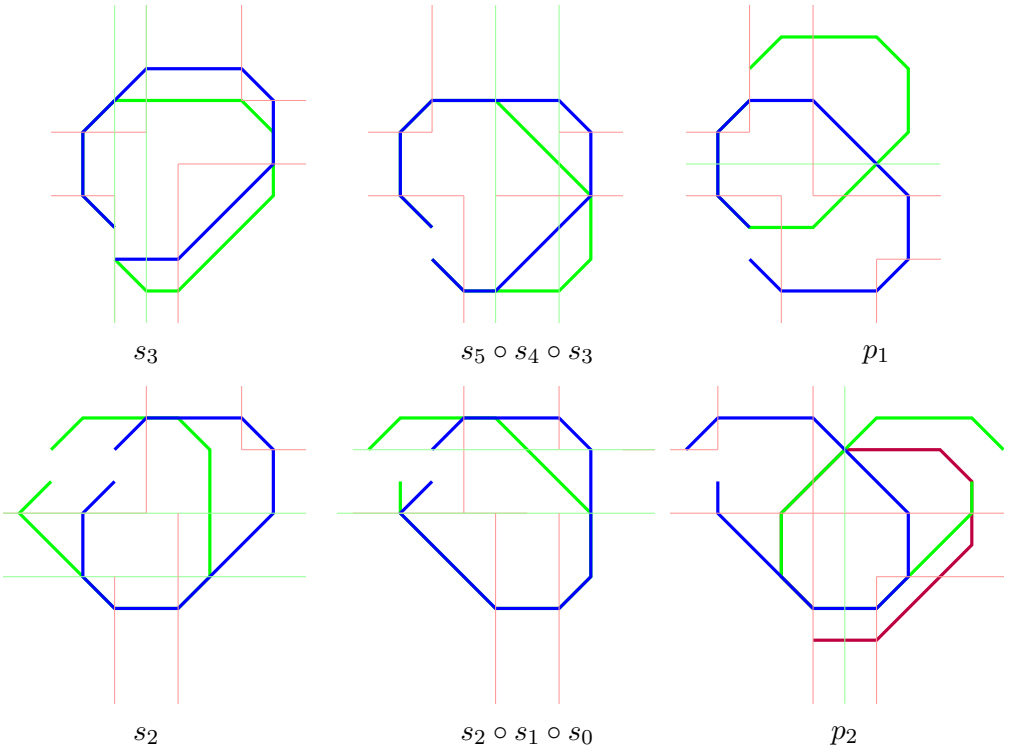


Figure 11. Starting with a single spiral, we show each significant step in the sequence (4.4). In blue, we show the result of previous transformations, in green is the result of the transformations listed below. In the last step, we also show the original spiral (in red).

To show that each step is an isomorphism of spiral diagrams, we have depicted the nontrivial steps in T on a typical spiral in Fig. 11.

We can present the nontrivial actions of these transformations as

$$
\begin{aligned}
&s_2\colon\ X \to X + \max(Y, B_3) - \max(Y, B_1),\\
&s_2\colon\ A_1 \to A_1 + B_3 - B_1, \qquad s_2\colon\ A_2 \to A_2 + B_3 - B_1,\\
&s_3\colon\ Y \to Y + \max(X, A_3) - \max(X, A_1),\\
&s_3\colon\ B_1 \to B_1 + A_3 - A_1, \qquad s_3\colon\ B_2 \to B_2 + A_3 - A_1,\\
&p_1\colon\ Y \to B_3 + B_4 - Y, \qquad p_2\colon\ X \to A_3 + A_4 - X.
\end{aligned}
$$

The composition in (4.4) gives (3.2).

Remark 4.1. The above constitutes the action on a tropical biquadratic that does not satisfy the requirement that the image under Π is a tropical cubic plane curve. A cubic plane curve may be obtained by applying ι_{A_4}, which has the effect of removing the ray given by L_4 and adding a ray given by the same formula, but pointing downward instead of upwards. Up to translational invariance, this is equivalent to the polygon considered in Section 5.7. In particular, their groups of transformations are of the same affine Weyl type.

An aspect of defining the group of transformations for a polygon or spiral diagram that we have not introduced in the above example is that we may always remove two parameters by taking into account uniqueness of a group of transformations up to translational equivalence. We can take this into account by insisting that two rays, of different asymptotic forms, pass through the origin. This means that we will often compose one of the above types of transformation with a translation so that any ray which is supposed to pass through the origin does so after

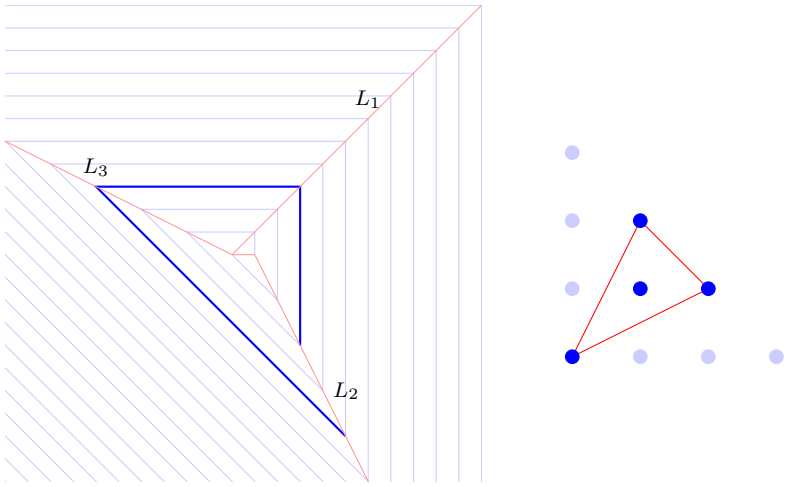


Figure 12. The spiral diagram for the system with affine Weyl symmetry of type $A_0^{(1)}$.

the transformation. This fixes a representation based on which rays we choose to pass through the origin.

5 Tropical representations of affine Weyl groups

While the task of finding subtraction free versions of the Cremona transformations in Sakai's list was presented (but not published) by Kajiwara et al. [18], what we wish to present is a different perspective. The derivation of the following list of affine Weyl representations will sometimes be a slightly different parameterization of the transformations of [18] due to the manner in which they were derived. We will also provide some of the geometric motivation behind our choices of generators. To this end, we shall display a spiral diagram and a nontrivial translation for each of the cases in Table 1. When the Newton polygon is known, this will also accompany the spiral diagram on the right.

5.1 Triangles

At the bottom of the hierarchy of multiplicative surfaces in [47] is the system with a symmetry of the dihedral group of order 6, which admits the presentation

$$\mathcal{D}_6 = \langle p_1, p_2 \colon\ p_1^3 = p_2^2 = (p_2 p_1)^2 = 1 \rangle.$$

This is the group permuting the three rays in Fig. 12. The rays may be parameterized by the equations

$$L_1 \colon\ Y - X - A = 0, \qquad L_2 \colon\ 2X + Y - B = 0, \qquad L_3 \colon\ X + 2Y - C = 0.$$

By exploiting scaling (i.e., $X \to X + \lambda$ and $Y \to Y + \mu$), we can reduce this to the case where we fix $B = C = 0$.

In this way, let p_1 permute the lines so that $p_1 \colon (L_1, L_2, L_3) \to (L_3, L_1, L_2)$. Similarly, p_2 is the transformation that swaps L_2 and L_3 via a reflection around the line $Y = X$. These are explicitly given by the piecewise linear transformations

$$\begin{aligned} &p_1 \colon\ X \to -X - Y - \frac{A}{3}, && p_2 \colon\ Y \to X + \frac{2A}{3}, && p_2 \colon\ A \to A, \\ &p_2 \colon\ X \to Y, && p_2 \colon\ X \to Y, && p_2 \colon\ A \to -A. \end{aligned}$$

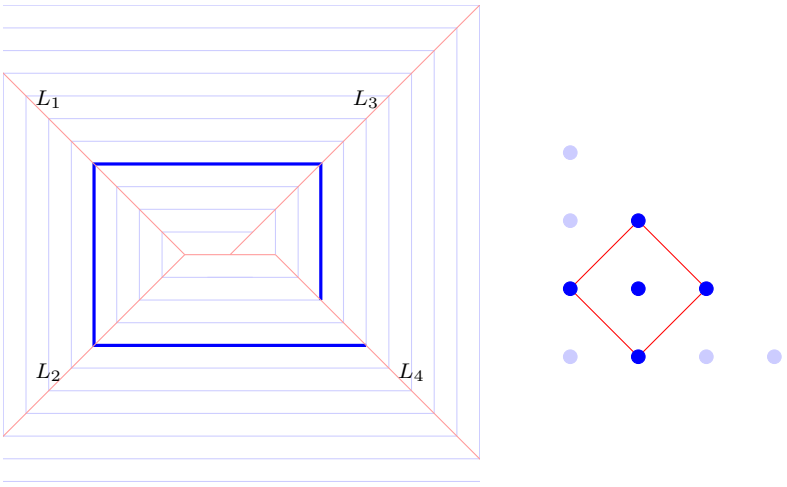


Figure 13. The spiral diagram for the system with affine Weyl symmetry of type $A_1^{(1)}$ with an additional dihedral symmetry.

As a very degenerate case, the transformations are simple given by (up to translations) a subgroup of actions of the type (4.2).

It is natural to see that $Q = A$. The limit which gives a fibration by tropical biquadratics is the limit as $A = Q = 0$. The resulting polygons arise as level sets of

$$H(X, Y) = \max(-X - Y, X, Y).$$

As the dihedral group, $\mathcal{D}_6$, contains no elements of infinite order, there is no difference equation associated with this group.

5.2 Rectangles

We consider a spiral diagram of quadralaterals which gives an affine Weyl group of type $W(A_1^{(1)})$ with an additional $\mathcal{D}_8$ symmetry. In the same way as above, we may exploit scaling so that the rays extending towards $X = -\infty$ pass through the origin. We paramaterize our rays as follows:

$$\begin{aligned} &L_1\colon\ Y + X = 0, \qquad && L_3\colon\ Y - X - A = 0,\\ &L_2\colon\ Y - X = 0, \qquad && L_4\colon\ Y + X - B = 0. \end{aligned}$$

This is depicted in Fig. 13.

The symmetry group for this system is the semidirect product of $\mathcal{D}_8 = \langle p_1, p_2\rangle$ and $W\big(A_1^{(1)}\big) = \langle s_0, s_1\rangle$. A presentation is given by

$$\mathcal{D}_8 \ltimes W\big(A_1^{(1)}\big) = \big\langle p_1, p_2, s_0, s_1\colon\ p_1^4 = p_2^2 = (p_1p_2)^2 = s_0^2 = s_1^2 = s_0p_2s_1p_2 = 1\big\rangle,$$

where the action of $\mathcal{D}_8$ is specified up to translation by a clockwise rotation of the four defining lines, p_1, whereas p_2 swaps L_3 and L_4. We write these transformations as

$$\begin{aligned} &p_1\colon\ X \to Y + \frac{B}{2}, && p_1\colon\ Y \to -X - \frac{B}{2}, && p_1\colon\ A \to B, && p_1\colon\ B \to A,\\ &p_2\colon\ X \to X, && p_2\colon\ Y \to -Y, && p_2\colon\ A \to -B, && p_2\colon\ B \to -A. \end{aligned}$$

Let s_0 be the conjugation of the transformation depicted in Fig. 7 with the piecewise linear transformation that makes L_2 and L_3 parrellel to the y-axis (and L_1 and L_4 to the x-axis). The transformation s_1 may be obtained in a similar manner with L_1 and L_4, giving

$$s_0\colon\ X \to X + \max(0, Y - X + A) - \max(0, Y - X) - \frac{A}{2},$$

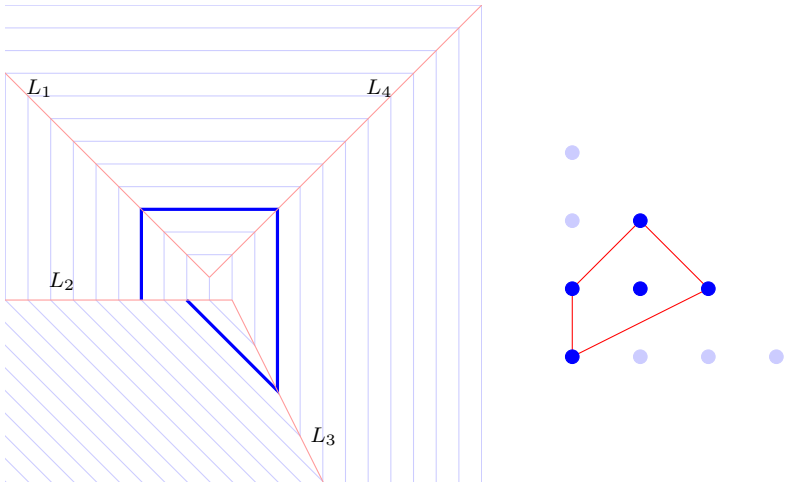


Figure 14. The spiral diagram for the system with affine Weyl symmetry $A_1^{(1)}$.

$$s_0\colon\ Y \to Y + \max(0, Y - X + A) - \max(0, Y - X) + \frac{A}{2},$$
$$s_0\colon\ A \to -A, \qquad s_0\colon\ B \to B - 2A,$$

and $s_1 = p_2 \circ s_0 \circ p_2$, which we write as

$$s_1\colon\ X \to X + \max(0, -X - Y - B) - \max(0, -X - Y) + \frac{B}{2},$$
$$s_1\colon\ Y \to Y + \max(0, -X - Y) - \max(0, -X - Y - B) + \frac{B}{2},$$
$$s_1\colon\ A \to A - 2B, \qquad s_1\colon\ B \to -B.$$

We find that $Q = A - B$ by tracing around the spiral. When $A = B$, we obtain the invariant

$$H(X, Y) = \max(-X, -Y, Y, X - A).$$

For the element $T = s_1 \circ s_0$, we resort to co-ordinates U and V, where $X = (U + V)/2$ and $Y = (U - V)/2$. The dynamical system in these variables is

$$\tilde{U} - U = B + 2\max(A, A + V) - 2\max(0, V),$$
$$\tilde{V} - V = 3A + 2\max(0, \tilde{U}) - 2\max(B, 2A + \tilde{U}),$$
$$T\colon\ A \to A + 2Q, \qquad T\colon\ A \to A - 2Q,$$

where $\tilde{U} = T(U)$ and $\tilde{V} = T(V)$.

5.3 Quadralaterals

We have another quadralateral that does not possess an additional dihedral symmetry. We break the dihedral symmetry by fixing the parameterization of the four rays in the following manner:

$$L_1\colon\ Y + X = 0, \qquad L_3\colon\ Y + 2X - A = 0,$$
$$L_2\colon\ Y = 0, \qquad L_4\colon\ Y - X - B = 0,$$

as depicted in Fig. 14.

The group of transformations that preserves this spiral diagram is of type

$$W(A_1^{(1)}) = \langle s_0, s_1\colon\ (s_0)^2 = (s_1)^2 \rangle,$$

where $s_1 \circ s_0$ is the element of infinite order. The first transformation, s_0, swaps the roles of L_1 with L_2 and L_3 with L_4, which we write as

$$\begin{aligned} &s_0\colon\ Y \to -Y - X, \qquad && s_0\colon\ A \to -B,\\ &s_0\colon\ X \to X, && s_0\colon\ B \to -A. \end{aligned}$$

The other involution, s_1, is a reflection around $X = B/2$ above $Y = 0$ (so that L_4 is sent to L_1) and a skewed reflection below $Y = 0$, given by $X \to -Y - X - B/2$, which simplifies to the following tropically rational transformation

$$\begin{aligned} &s_1\colon\ X \to \max(0, -Y) - X - B, \qquad && s_1\colon\ A \to -2B - A,\\ &s_1\colon\ Y \to Y, && s_1\colon\ B \to B. \end{aligned}$$

This is simply the conjugation of ι_0 with a swap of X and Y. We find $Q = A + B$ by tracing around one spiral. When $A = -B$, we obtain the invariant

$$H(X, Y) = \max(-X - Y, -X, Y, X - A).$$

The composition, $T = s_1 \circ s_0$, gives the evolution equations

$$\begin{aligned} &\tilde{X} + X = \max(0, Y + X) + A,\\ &\tilde{Y} + Y = -X,\\ &T\colon\ A \to A + Q, \qquad && T\colon\ B \to B - Q. \end{aligned}$$

This element, T, is the generator for $\mathbb{Z}$ in the decomposition of $W(A_1^{(1)}) \cong \mathbb{Z} \ltimes \mathfrak{G}_2$ in [18, 47]. Alternatively, we could write this system as a second order difference equation in $W = -Y$, where the resulting system becomes

$$W + 2\tilde{W} + \tilde{\tilde{W}} = \max(0, \tilde{W}) + A,$$

which coincides with a more standard version of an ultradiscrete version of the first Painlevé equation [43].

5.4 Pentagons

This case is associated with u-$\mathrm{P_{II}}$. To preserve much of the structure of the two previous cases, we have parameterize the five rays as follows:

$$\begin{aligned} &L_1\colon\ Y + X - A = 0, \qquad && L_4\colon\ Y + X - B = 0,\\ &L_2\colon\ Y = 0, && L_5\colon\ Y - X - C = 0,\\ &L_3\colon\ X = 0, \end{aligned}$$

as depicted in Fig. 15.

A presentation of the group of transformations is

$$A_1^{(1)} \times A_1^{(1)} = \langle s_0, s_1, w_0, w_1\colon\ s_i^2 = w_i^2 = 1 \rangle,$$

where s_0 is a reflection around the line $Y = X$, and s_1 is the same the action of s_1 in the previous section in that above the line $Y = 0$, we have a reflection, and below the line, we skew the plane. The generators are

$$s_0\colon\ X \to Y, \qquad p_0\colon\ A \to B, \qquad p_0\colon\ C \to -C,$$

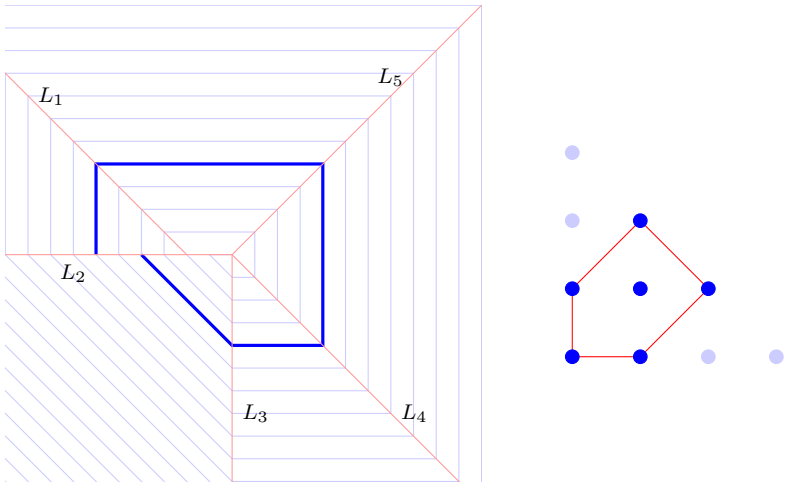


Figure 15. The pentagon.

$$\begin{aligned}
&s_0\colon\ Y \to X, && p_0\colon\ B \to A,\\
&s_1\colon\ X \to \max(0,-Y) - X + B, && p_1\colon\ A \to B + C, \qquad p_1\colon\ A_2 \to A - B,\\
&s_1\colon\ Y \to Y, && p_1\colon\ B \to B.
\end{aligned}$$

As for the other part of the group, w_0 swaps L_1 and L_4 via a transformation that sheers between the lines L_1 and L_4, which can be written as

$$\begin{aligned}
&w_0\colon\ X \to X + \max(0, X + Y - A) - \max(0, X + Y - B),\\
&w_0\colon\ Y \to Y + \max(0, X + Y - B) - \max(0, X + Y - A),\\
&w_0\colon\ A \to B, \qquad w_0\colon\ B \to A, \qquad w_0\colon\ C \to C + 2A - 2B,
\end{aligned}$$

while w_1 is a piecewise linear sheering transformation swapping L_2 and L_3, which we write as

$$\begin{aligned}
&w_1\colon\ X \to X + C + \max(0, X, Y - C) - \max(0, X, Y),\\
&w_1\colon\ X \to Y + \max(C, X, Y - C) - \max(0, X, Y),\\
&w_1\colon\ A_0 \to A + C, \qquad w_1\colon\ B \to B + C, \qquad s_1\colon\ C \to -C.
\end{aligned}$$

Tracing around the figure reveals that Q is given by

$$Q = B + C - A.$$

When $C = A - B$, we obtain the invariant

$$H(X, Y) = \max(-X - Y, -X, -Y, X - B, Y - A).$$

One simple translation is the composition, $T = (s_0 \circ s_1)^2$, which can be written as

$$\tilde{X} + X = \max(0, -Y) + B, \tag{5.1a}$$

$$\tilde{Y} + Y = \max(0, -\tilde{X}) + B + C, \tag{5.1b}$$

$$T\colon\ A \to A + Q, \qquad T\colon\ B \to B + Q, \tag{5.1c}$$

where the other obvious translation, $(w_0 \circ w_1)$, commutes with T. This system is called u-$\mathrm{P_{II}}$. Exact solutions of (5.1) were studied in [26].

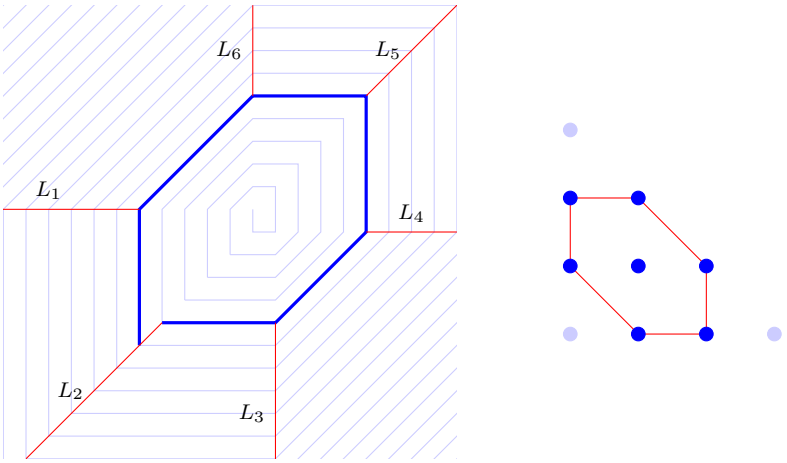


Figure 16. The spiral diagram for the discrete Painlevé equation with $A_2^{(1)} + A_1^{(1)}$ symmetry.

5.5 Hexagons

The tropical representation for $W(A_2^{(1)} + A_1^{(1)})$ was one of the first to be written down [19]. There are a number of equivalent ways of obtaining a hexagon as a cubic plane curve, we choose to parameterize our rays so that our presentation coincides with the presentation of Noumi et al. [19]. In particular, our rays are parameterized as follows:

$$\begin{aligned} &L_1\colon\ Y = 0, && L_4\colon\ Y - B_2 = 0,\\ &L_2\colon\ Y - X - B_1 = 0, && L_5\colon\ Y - X + A_0 - B_1 = 0,\\ &L_3\colon\ X = 0, && L_6\colon\ X + A_1 = 0, \end{aligned}$$

which is depicted in Fig. 16.

The group of transformations preserving these spiral diagrams is of the affine Weyl type

$$W\big(A_2^{(1)} + A_1^{(1)}\big) = \big\langle s_0, s_1, s_2, r_0, r_1\colon\ s_i^2 = r_i^2 = (s_i s_{i+1})^3 \big\rangle.$$

We have a natural $A_2^{(1)}$ group acting on the pairs of lines opposite to each other, in particular, if we denote the piecewise linear transformation that shears the space between two lines (as in Fig. 7), L_i and L_j, by $\sigma_{i,j}$, then we let $s_0 = \sigma_{2,5}$, $s_1 = \sigma_{3,6}$ and $s_2 = \sigma_{1,4}$. The action of these elements may be written as

$$\begin{aligned} &s_0\colon\ X \to X + \max(X + B_1, Y) - \max(B_1 + X, A_0 + Y),\\ &s_0\colon\ Y \to A_0 + Y + \max(X + B_1, Y) - \max(B_1 + X, A_0 + Y),\\ &s_1\colon\ X \to A_1 + X, \qquad s_1\colon\ Y \to Y + \max(0, A_1 + X) - \max(0, X),\\ &s_2\colon\ X \to X + \max(A_2, Y) - A_2 - \max(0, Y), \qquad s_2\colon\ Y \to Y - A_2, \end{aligned}$$

where the action on the parameters is

$$s_i\colon\ A_i \to -A_i, \qquad s_i\colon\ A_j \to A_j - 2A_i.$$

The action of the $W\big(A_1^{(1)}\big) = \langle r_0, r_1 \rangle$ component is as follows:

$$\begin{aligned} r_0\colon\ X \to{}& X + \max(X, X + Y - A_2, Y - A_1 - A_2)\\ &- \max(X, A_0 - B_1 + Y, A_0 + A_1 - B_1 + X + Y),\\ r_0\colon\ Y \to{}& Y + \max(X, X + Y - A_2, Y - A_1 - A_2) \end{aligned}$$

$$- \max(X, A_0 - B_1 + Y, A_0 + A_1 - B_1 + X + Y),$$
$$r_1 \colon\ X \to X + \max(X + B_1, Y, B_1) - \max(X, Y, 0),$$
$$r_1 \colon\ Y \to Y + \max(X, Y - B_1, -B_1) - \max(X, Y, 0).$$

The Dynkin diagram automorphisms comprise of a reflection around L_2, which swaps L_1 with L_3 and another that swaps L_4 with L_6, and hence, are given by

$$p_1 \colon\ A_{0,1,2} \to A_{1,2,0}, \qquad p_1 \colon\ B_{0,1} \to B_{1,0},$$
$$p_1 \colon\ X \to Y - A_2, \qquad p_1 \colon\ Y \to A_0 - B_1 + Y - X,$$
$$p_2 \colon\ A_{0,1,2} \to -A_{0,2,1}, \qquad p_2 \colon\ B_{0,1} \to -B_{1,0},$$
$$p_2 \colon\ X \to A_2 - Y, \qquad p_2 \colon\ Y \to -A_1 - X.$$

These generators have been chosen to coincide with the original presentation of Noumi et al. [19]. The transformations p_1 and p_2 satisfy the relations

$$p_1^3 = p_2^2 = p_1^{-1} \circ s_{i+1} \circ p_1 \circ s_i = p_2 \circ r_{i+1} \circ p_1 \circ r_i = 1.$$

We find the value of Q is

$$Q = A_0 + A_1 + A_2 = B_0 + B_1,$$

which, when $Q = 0$, gives invariant curves arising as the level sets of

$$H(X, Y) = \max(-A_1 - B_1 - X, X, A_2 - Y, A_2 + X - Y, Y - B_1, Y - A_1 - B_1 - X).$$

We have two distinct evolution equations corresponding to different lattice directions. Firstly, we have the translation $T_1 = p_1 \circ s_2 \circ s_1$, which sends (X, Y) to $(\tilde{X}, \tilde{Y})$, related via

$$\tilde{X} - Y = B_0 + \max(B_1 + X, Y) - \max(X + A_1 + A_2, Y + B_0),$$
$$\tilde{Y} - Y + X = A_0 + A_2 - B_1 + \max(\tilde{X}, 0) - \max(\tilde{X}, A_0 + A_2),$$
$$T_1 \colon\ A_0 \to A_0 + Q, \qquad T_1 \colon\ A_1 \to A_1 - Q,$$

which corresponds to a version of u-$\mathrm{P_{III}}$ [19]. Secondly, we have $T_2 = p_2 \circ r_0$, which sends (X, Y) to $(\hat{X}, \hat{Y})$, where

$$\hat{X} + Y = B_1 + A_2 + \max(0, X, Y) - \max(0, Y, X + B_1),$$
$$\hat{Y} + X = A_0 - B_0 + \max(0, X, Y) - \max(B_1, Y, X + B_1),$$
$$T_2 \colon\ B_0 \to B_0 + Q, \qquad T_2 \colon\ B_1 \to B_1 - Q.$$

which corresponds to a version of u-$\mathrm{P_{IV}}$ [19].

5.6 Septagons

This case is associated with u-$\mathrm{P_V}$ [43]. There are seven rays, specified as follows:

$$L_1 \colon\ Y = 0, \qquad L_4 \colon\ X = 0,$$
$$L_2 \colon\ Y - B_0 = 0, \qquad L_5 \colon\ X - B_3 = 0,$$
$$L_3 \colon\ Y + B_1 = 0, \qquad L_6 \colon\ X + B_4 = 0,$$
$$L_7 \colon\ Y - X + B_1 + B_2 + B_3 + B_4 = 0,$$

which we depict in Fig. 17.

The group of transformations is of affine Weyl type

$$W\big(A_4^{(1)}\big) = \langle s_0, \ldots, s_4 \rangle.$$

Rather than writing each relation, a presentation may be derived from the groups corresponding Dynkin diagram, which is shown below:

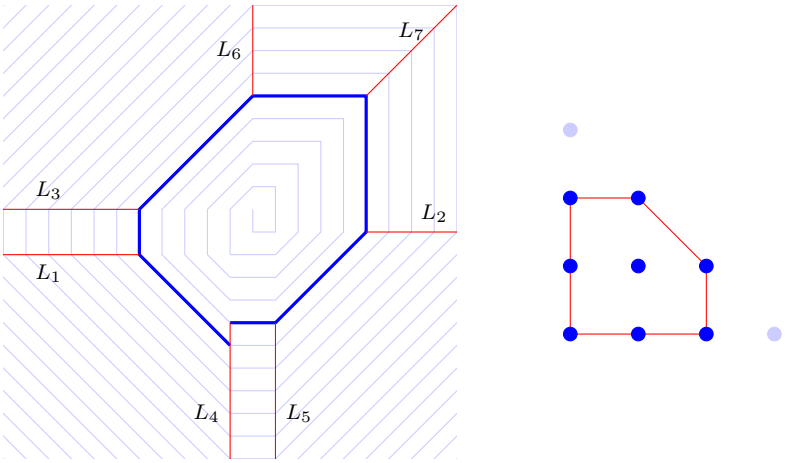
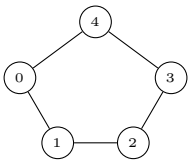


Figure 17. The spiral diagram for the case of the ultradiscrete Painlevé equation with $A_4^{(1)}$ symmetry.



From the Dynkin diagram, the action of s_i on is specified by

$$s_i\colon\ B_j = \begin{cases} -B_i & \text{if } i = j, \\ B_j + B_i & \text{if } i \neq j \text{ and node } i \text{ is adjacent to node } j, \\ B_j & \text{otherwise.} \end{cases} \tag{5.2}$$

From this point, we will choose parameterizations of rays so that that the action of s_i on the parameters determined by the Dynkin diagram in this way.

The first action is one that interchanges L_1 and L_2 by the piecewise linear shearing transformation

$$s_0\colon\ X \to X + \max(Y, B_0) - B_0 - \max(0, Y), \qquad s_0\colon\ Y \to Y - B_0.$$

The second transformation is a simple translation,

$$s_1\colon\ Y \to Y + B_1,$$

which has the effect of moving L_3 to L_1, hence, redefining L_1 and L_3. The transformation s_2 has the form

$$\begin{aligned} &s_2\colon\ X \to X + \max(B_2, B_2 + X, Y) - \max(0, X, Y), \\ &s_2\colon\ Y \to Y + \max(0, B_2 + X, Y) - B_2 - \max(0, X, Y), \end{aligned}$$

while s_3 simply is a translation in X that redefines L_4 and is given by

$$s_3\colon\ X \to X - B_3.$$

The last transformation is similar to s_0, but applied to the lines L_4 and L_5,

$$s_4\colon\ X \to B_4 + X, \qquad s_4\colon\ Y \to \max(-X, B_4) - Y,$$

The Dynkin diagram automorphisms are generated by a rotation of the nodes

$$p_1\colon\ B_i \to B_{i+1}, \qquad p_1\colon\ X \to \max(0,X,Y) - X - Y, \qquad p_1\colon\ Y \to \max(0,X) - Y,$$

and a reflection

$$p_2\colon\ B_{0,1,2,3,4} \to -B_{2,1,0,4,3}, \qquad p_2\colon\ Y \to \max(0,X) - Y,$$

Tracing around the parameters provides the variable, Q, given by

$$Q = B_0 + B_1 + B_2 + B_3 + B_4.$$

In the autonomous limit, when $Q = 0$, the spiral diagram degenerates to a foliation by tropical cubic plane curves, specified by the level sets of

$$\begin{aligned} H(X,Y) = \max\big(&Y, \max(0,B_1) - B_1 - B_4 - X, Y - B_4 - X,\\ &\max(0,B_3) - B_1 - B_3 - B_4 - Y, -B_1 - B_4 - X - Y,\\ &X - B_1 - B_3 - B_4 - Y\big). \end{aligned}$$

The translation expressed as the composition

$$T = s_4 \circ s_3 \circ s_2 \circ s_1 \circ p_1,$$

corresponds to the evolution equation

$$\begin{aligned} &\tilde{X} + X = B_3 + \max(0,\tilde{Y}) + \max(0,\tilde{Y} + B_1) - \max(B_0, Q + \tilde{Y}),\\ &\tilde{Y} + Y = -B_1 - B_3 + \max(0,X) + \max(A_3,X) - \max(0,X + B_4),\\ &T\colon\ A_0 \to A_0 - Q, \qquad T\colon\ A_4 \to A_4 + Q, \end{aligned}$$

which is known as the ultradiscrete version of the fifth Painlevé equation [43].

5.7 Octagons

The biquadratic invariants obtained in the autonomous limit of q-$\mathrm{P_{VI}}$ in Section 3 are not naturally mapped to cubic plane curves. However, under a simple transformation, we can present an equivalent system based on octagons arising as cubic plane curves whose rays are parameterized as follows:

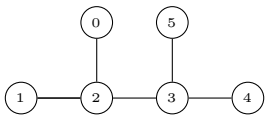
$$\begin{aligned} &L_1\colon\ X = 0, && L_5\colon\ Y = 0,\\ &L_2\colon\ X - B_2 = 0, && L_6\colon\ Y + B_5 = 0,\\ &L_3\colon\ X - B_1 - B_2 = 0, && L_7\colon\ Y - X - B_3 = 0,\\ &L_4\colon\ X + B_0 = 0, && L_8\colon\ Y - X - B_3 - B_4 = 0, \end{aligned}$$

which is depicted in Fig. 18

The group of transformations preserving these spiral diagrams is of affine Weyl type

$$W\big(D_5^{(1)}\big) = \langle s_0, \ldots, s_5 \rangle.$$

A presentation may be derived from the Dynkin diagram below:



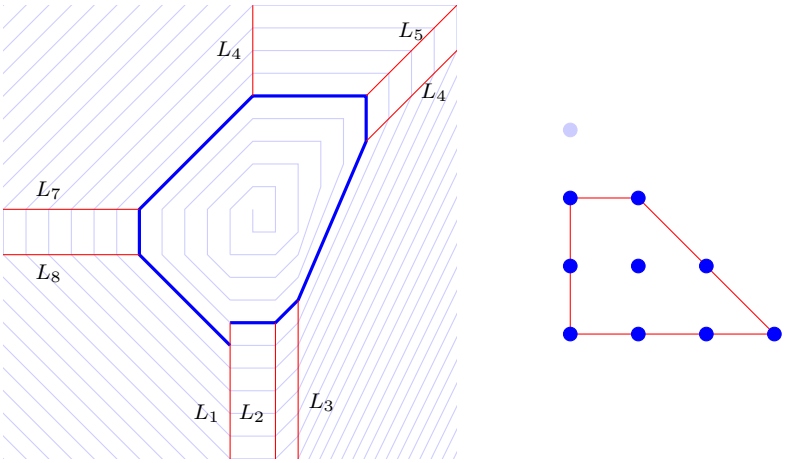


Figure 18. The spiral diagram for the case of the ultradiscrete Painlevé equation with $D_5^{(1)}$ symmetry.

We analogously specify the generators as we did before, where we denote the generators (in terms of $\sigma_{i,j}$ which swaps L_i with L_j),

$$s_0 = \sigma_{1,4}, \qquad s_1 = \sigma_{3,4}, \qquad s_2 = \sigma_{1,3},$$
$$s_3 = \sigma_{5,7}, \qquad s_4 = \sigma_{7,8}, \qquad s_5 = \sigma_{5,6}.$$

These generators may be written

$$\begin{aligned}
&s_0\colon\ X \to X + B_0, \qquad && s_0\colon\ Y \to Y + \max(0, X + B_0) - \max(0, X),\\
&s_2\colon\ X \to X - B_2, \qquad && s_5\colon\ Y \to Y + B_5,\\
&s_3\colon\ X \to X + \max(B_3 + \max(0, X), Y) - \max(0, X, Y),\\
&s_3\colon\ Y \to X + \max(0, X + B_3, Y) - \max(0, X, Y) - B_3,
\end{aligned}$$

and the Dynkin diagram automorphisms, p_1 and p_2, are

$$\begin{aligned}
&p_1\colon\ B_{0,1,2,3,4,5} \to -B_{5,4,3,2,1,0},\\
&p_1\colon\ X \to \max(0, X) - Y, && p_1\colon\ Y \to \max(0, X, Y) - X - Y,\\
&p_2\colon\ B_{0,1,2,3,4,5} \to -B_{0,1,2,3,5,4},\\
&p_2\colon\ X \to -X, && p_2\colon\ Y \to Y - X - B_3,
\end{aligned}$$

Tracing around the particular values gives us the variable

$$Q = B_0 + B_1 + 2B_2 + 2B_3 + B_4 + B_5$$

In particular, when $Q = 0$, we obtain the invariant

$$\begin{aligned}
H(X, Y) = \max\big(&\max(0, -B_5) - X, Y - X, \max(0, -B_1, -B_1 - B_2) - B_5 - Y,\\
&B_0 + Y, \max(0, -B_1, -B_1 - B_2) + X - B_2 - B_5 - Y, -b_5 - X - Y,\\
&B_0 + B_3 + \max(0, B_4) + X, 2X - Y - B_1 - 2B_2 - B_5\big).
\end{aligned}$$

The usual translation that is associated with the dynamics of u-$\mathrm{P_{VI}}$ and the symmetry QRT equation is the action of

$$T = p_2 \circ p_1 \circ p_2 \circ s_1 \circ s_2 \circ s_3 \circ s_5 \circ s_4 \circ s_3 \circ s_2 \circ s_1.$$

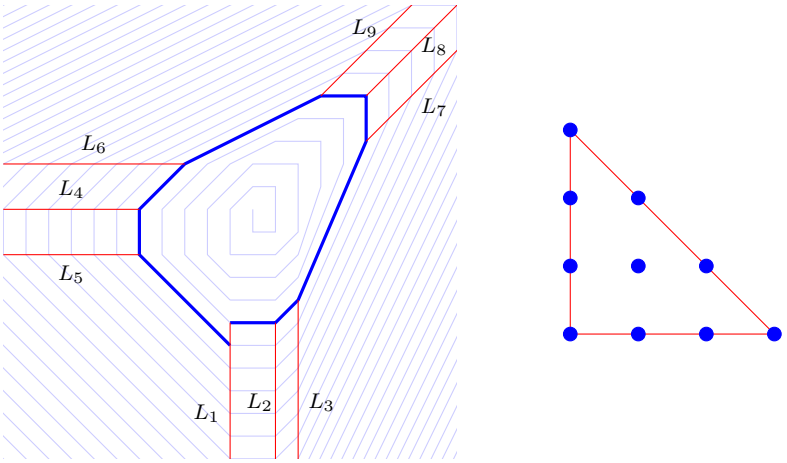


Figure 19. The spiral diagram for the case of the ultradiscrete Painlevé equation with $E_6^{(1)}$ symmetry.

To express the evolution of this system in a manner closer to that of (3.2), we invert the transformation that was used to express the invariant as a tropical cubic curve. This is done by letting

$$Z = \max(0, X) + \max(0, X - B_2) - \max(0, X + B_0) - Y,$$

which means the evolution in terms of X and Z is expressed as

$$\begin{aligned} X + \tilde{X} &= B_2 - B_5 + \max(0, Z) - \max(0, Z + B_0 + B_2 + B_3) \\ &\quad + \max(B_5, Z) - \max(0, Z + B_0 + B_2 + B_3 + B_4), \\ Z + \tilde{Z} &= B_5 - B_2 + \max(0, \tilde{X}) - \max(0, \tilde{X} + Q + B_0) \\ &\quad + \max(B_2, \tilde{X}) - \max(0, \tilde{X} + Q - B_1 - B_2), \end{aligned}$$

which is equivalent to (3.2) above.

5.8 Enneagons

It is at this point we go beyond the QRT maps defined by biquadratic cases [29, 46]. We exploit the translational freedom to parameterize two rays coincide with the y-axis and x-axis respectively. The remaining ray are parameterized as follows:

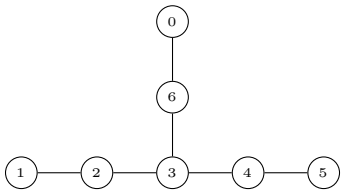
$$\begin{aligned} &L_1\colon\ X = 0, && L_6\colon\ Y + B_0 + B_6 = 0, \\ &L_2\colon\ X - B_2 = 0, && L_7\colon\ Y - X + B_3 = 0, \\ &L_3\colon\ X - B_1 - B_2 = 0, && L_8\colon\ Y - X + B_3 + B_4 = 0, \\ &L_4\colon\ Y = 0, && L_9\colon\ Y - X + B_3 + B_4 + B_5 = 0, \\ &L_5\colon\ Y + B_6 = 0. \end{aligned}$$

The relevant spiral diagram is of irregular enneagons, depicted in Fig. 19.

The group of transformations are of affine Weyl type

$$W\big(E_6^{(1)}\big) = \langle s_0, \ldots, s_6 \rangle.$$

The presentation, and action on the parameters, is specified by the Dynkin diagram below:



We may now parameterize the affine Weyl group actions by first specifying the generators that have a little effect on X and Y, by letting $s_0 = \sigma_{5,6}$, $s_1 = \sigma_{2,3}$, $s_2 = \sigma_{1,2}$, $s_4 = \sigma_{7,8}$, $s_5 = \sigma_{8,9}$ and $s_6 = \sigma_{4,5}$. In these cases, the effect on X and Y are trivial, except for s_2 and s_6, which have the effect

$$s_2\colon\ X \to X - B_2, \qquad s_6\colon\ Y \to Y + B_6.$$

The action of s_3 is given by

$$\begin{aligned} &s_3\colon\ X \to X + \max(B_3, B_3 + X, Y) - \max(0, X, Y),\\ &s_3\colon\ Y \to Y - B_3 + \max(0, B_3 + X, Y) - \max(0, X, Y). \end{aligned}$$

The Dynkin diagram automorphisms are given by

$$\begin{aligned} &p_1\colon\ B_{0,1,2,3,4,5,6} \to -B_{5,1,2,3,6,0,4},\\ &p_1\colon\ X \to -X, \qquad p_2\colon\ Y \to Y - X - B_3,\\ &p_2\colon\ B_{0,1,2,3,4,5,6} \to -B_{1,0,6,3,4,5,2},\\ &p_2\colon\ X \to Y, \qquad p_2\colon\ Y \to X. \end{aligned}$$

Tracing around the enneagon, we obtain the variable

$$Q = B_0 + B_1 + 2B_2 + 3B_3 + 2B_4 + B_5 + B_6.$$

In the autonomous limit, when $Q = 0$, this spiral diagram degenerates to give a fibration by cubic plane curves, which may be expressed as the tropical curves that arise as the level sets of

$$\begin{aligned} H(X,Y) = \max\big(&2X - Y - B_1 - B_2, \max(0, -B_2, -B_1 - B_2) + X - Y - B_2,\\ &\max(0, -B_5, -B_4 - B_5) + X - B_1 - 2B_2 - B_3, \max(0, -B_1, -B_2 - B_2) - Y,\\ &Y + \max(0, -B_4, -B_4 - B_5) - B_1 - 2B_2 - 2B_3 - B_4, 2Y + B_0 + 2B_6 - X,\\ &Y + B_6 + \max(0, B_0, B_0 + B_6) - X, \max(0, B_6, B_0 + B_6) - X, -X - Y\big). \end{aligned}$$

The translation that is associated with the dynamics of the discrete Painlevé equation in this case is given by

$$T = p_1 \circ p_2 \circ s_1 \circ s_2 \circ s_3 \circ s_4 \circ s_6 \circ s_0 \circ s_3 \circ s_2 \circ s_1 \circ s_6 \circ s_3 \circ s_2 \circ s_4 \circ s_3 \circ s_6 \circ s_0.$$

Though the evolution equation is very complicated, the action can be evaluated quite easily by the geometric method in [16]. In the case of a tropical cubic genus one curve, the action of T can be describes as follows: we choose two two rays, say L_i and L_j, and let T move L_i to the point in which the other rays and $T(L_i)$ define a pencil of tropical cubic genus one curves that foliate the plance, i.e., rather than spirals, we have closed curves. Any point, $P \in \mathbb{TP}_2$, is now on some closed genus one cubic curve, C, in the pencil. We send P to $T(P)$, so that $T(P)$ satisfies

$$T(P) + T(L_i) = P + L_j, \tag{5.3}$$

where we interpret $T(L_i)$ and L_i in terms of the unique stable intersection of $T(L_i)$ and L_j with C respectively and the addition is in accordance with the group law on C (see [5]). Finally we send L_j to a point in which $T(L_j)$ satisfies

$$L_i + L_j = T(L_i) + T(L_j),$$

on C. We have illustrated this in Fig. 20.

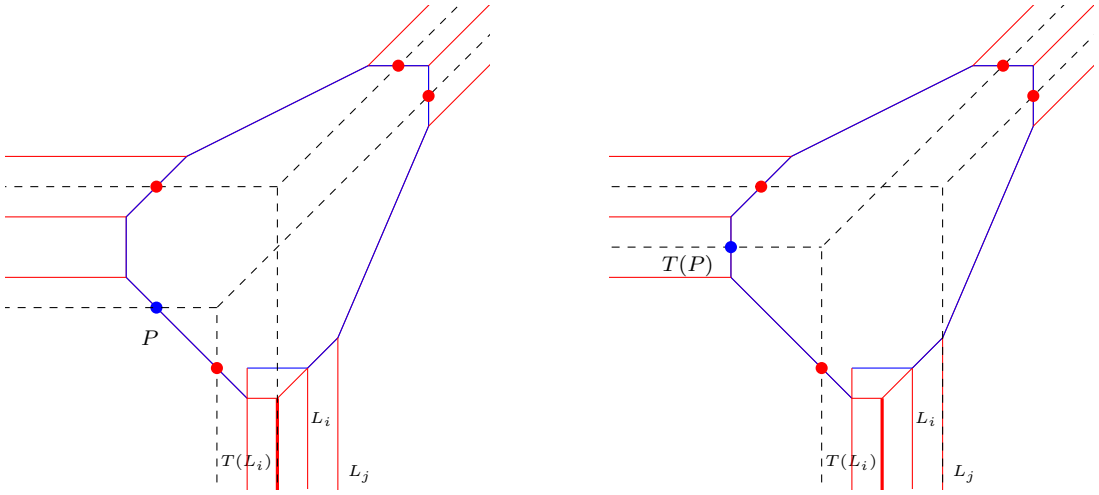


Figure 20. This is a pictorial represection of (5.3) where the dashed lines intersect the polygon at the four fixed points (in red) and P and $T(L_i)$ on the left and $T(P)$ and L_j on the right.

5.9 Decagons

The rational surface of type $A_1^{(1)}$ was obtained by blowing up three points on a line and six on a quadratic curve [47]. The resulting surface is rationally equivalent to the surface obtained by blowing up four points at lines at infinity and two points at on the third line at infinity. Hence, in the discrete setting, the underlying surface and the symmetries $W\big(E_7^{(1)}\big)$ obtained here are equivalent up to a rational transformation to those of [47].

The most general tropical cubic plane curve is a enneagon, hence, to describe the decagon spirals, we need to consider spiral degenerations of quartic plane curves with two rays of order two. We choose to parameterize these rays as follows:

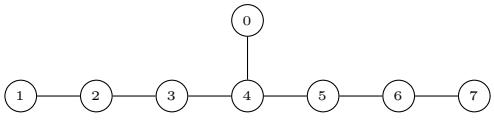
$$
\begin{aligned}
&L_1\colon\ X + B_4 = 0, && L_5\colon\ Y = 0,\\
&L_2\colon\ X + B_4 + B_5 = 0, && L_6\colon\ Y - B_3 = 0,\\
&L_3\colon\ X + B_4 + B_5 + B_6 = 0, && L_7\colon\ Y - B_3 - B_2 = 0,\\
&L_4\colon\ X + B_4 + B_5 + B_6 + B_7 = 0, && L_8\colon\ Y - B_3 - B_2 - B_1 = 0,\\
&L_9\colon\ Y - X - B_0 = 0, && L_{10}\colon\ Y - X = 0.
\end{aligned}
$$

It should be noted that L_9 and L_{10} are of order 2. With these considerations, the resulting system of spiraling polygons is depicted in Fig. 21.

The resulting group of transformations is of affine Weyl type

$$W\big(E_7^{(1)}\big) = \langle s_0, \dots, s_7 \rangle.$$

This groups Dynkin diagram is below:



The reflections are given by $s_0 = \sigma_{9,10}$, $s_1 = \sigma_{7,8}$, $s_2 = \sigma_{6,7}$, $s_3 = \sigma_{5,6}$, $s_5 = \sigma_{1,2}$, $s_6 = \sigma_{2,3}$ and $s_7 = \sigma_{3,4}$, hence, the nontrivial actions are given by

$$s_0\colon\ X \to X + B_0, \qquad s_3\colon\ Y \to Y + B_3, \qquad s_3\colon\ X \to X + B_3,$$

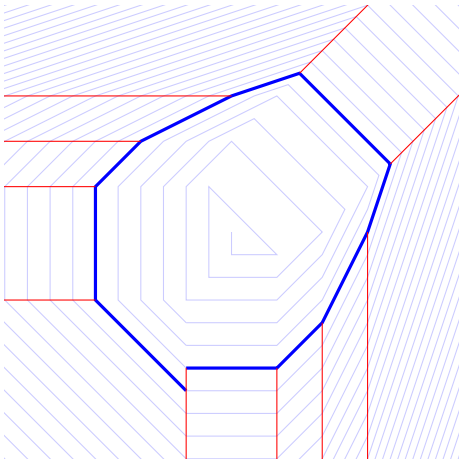


Figure 21. A spiral diagram for the $E_7^{(1)}$ case.

$$
\begin{aligned}
&s_4\colon\ X \to X - B_4 + \max(B_4, X, Y) - \max(B_4, X, B_4 + Y),\\
&s_4\colon\ Y \to Y + \max(0, X, Y) - \max(B_4, X, B_4 + Y).
\end{aligned}
$$

We also have a single Dynkin diagram automorphism. This Dynkin diagram automorphism has the effect of sending X to $-X$, and Y to $-Y$, which swaps all the eight first order rays, however, it also has the effect of reflecting the two rays, L_9 and L_{10}, in opposite direction, hence, we compose this a transformation of the form of ι_A along L_9 and L_{10}, giving

$$
\begin{aligned}
&p_1\colon\ X \to Y + B_4 - \max(Y, X) - \max(Y, B_0 + X),\\
&p_1\colon\ Y \to X + B_0 + B_4 - \max(Y, X) - \max(Y, B_0 + X),\\
&p_1\colon\ B_{0,1,2,3,4,5,6,7} \to B_{0,7,6,5,4,3,2,1}.
\end{aligned}
$$

Tracing around the spirals reveals that

$$
Q = 2B_0 + B_1 + 2B_2 + 3B_3 + 4B_4 + 3B_5 + 2B_6 + B_7,
$$

which in the autonomous limit, when $Q = 0$, gives a closing of spirals to give the following invariant

$$
\begin{aligned}
H(X, Y) = \max\big(&0, Y + \mu_1, 2Y + \mu_2, X + \mu_5, 2X + \mu_6,\\
&\max(Y + \mu_3, X - B_0 + \mu_7) + \max(Y, X + B_0) + \max(X, Y),\\
&2\max(Y, X + B_0) + 2\max(X, Y) + \mu_4\big) - X - Y,
\end{aligned}
$$

where the values of μ_i are defined by

$$
\begin{aligned}
&\max(0, X) + \max(0, B_3 + X) + \max(0, B_3 + B_2 + X)\\
&\qquad + \max(0, B_3 + B_2 + B_1 + X) = \max(0, \mu_1 + X, \mu_2 + 2X, \mu_3 + 3X, \mu_4 + 4X),\\
&\max(0, X - B_4) + \max(0, X - B_4 - B_5) + \max(0, X - B_4 - B_5 - B_6)\\
&\qquad + \max(0, X - B_4 - B_5 - B_6 - B_7) = \max(0, \mu_5 + X, \mu_6 + 2X, \mu_7 + 3X, \mu_8 + 4X).
\end{aligned}
$$

A translation associated with the ultradiscrete Painlevé equation is given by

$$
\begin{aligned}
T = {}& p_1 \circ s_1 \circ s_2 \circ s_3 \circ s_4 \circ s_0 \circ s_5 \circ s_4 \circ s_3 \circ s_2 \circ s_1 \circ s_6 \circ s_5 \circ s_4 \circ s_0\\
&\circ s_3 \circ s_2 \circ s_4 \circ s_3 \circ s_5 \circ s_4 \circ s_0 \circ s_6 \circ s_5 \circ s_4 \circ s_3 \circ s_2 \circ s_1,
\end{aligned}
$$

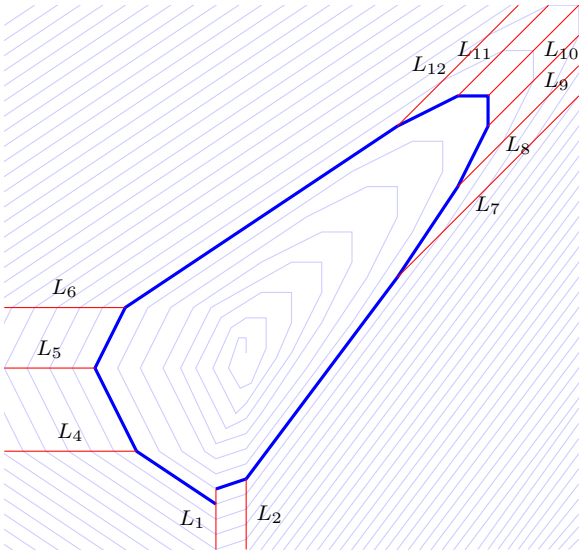


Figure 22. A spiral diagram for the $E_8^{(1)}$ case.

whose action on $\mathbb{T}^2$ is too complicated to be written here. However, the action of T may be described by the theory of [16], where the evolution takes the form

$$T(P) + T(L_i) = P + L_j, \tag{5.4}$$

where the addition here is defined in terms of the group law on a tropical quartic genus one curve.

5.10 Undecagon

The blow-up points in the original classification of Sakai [47] on $\mathbb{P}_2$ lie on a single nodal cubic. This configuration is birationally equivalent (by a series of blow-ups and blow-downs) to a configuration in $\mathbb{P}_2$ in which there are three order two singularities on the line at $y = 0$, two order three singularities on the line $x = 0$ and six order one singularities on the line $z = 0$. Hence, in the discrete setting, the underlying surface and the symmetries of affine Weyl type $E_8^{(1)}$ obtained here are equivalent up to a rational transformation to those of [47].

The tropical analogue requires we have a configuration of two, three and six rays, which may be parameterized as follows:

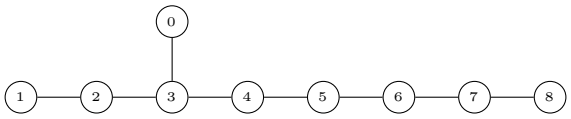
$$\begin{aligned}
&L_1\colon\ X = 0, && L_7\colon\ Y - X - B_3 - B_4 = 0,\\
&L_2\colon\ X - B_0 = 0, && L_8\colon\ Y - X - B_3 - B_4 - B_5 = 0,\\
&L_3\colon\ Y = 0, && L_9\colon\ Y - X - B_3 - B_4 - B_5 - B_6 = 0,\\
&L_4\colon\ Y + B_2 = 0, && L_{10}\colon\ Y - X - B_3 - B_4 - B_5 - B_6 - B_7 = 0,\\
&L_5\colon\ Y + B_1 + B_2 = 0, && L_{11}\colon\ Y - X - B_3 - B_4 - B_5 - B_6 - B_7 - B_8 = 0,\\
&L_6\colon\ Y - X - B_3 = 0,
\end{aligned}$$

where L_1 and L_2 are of order 3, L_4, L_5 and L_6 are of order 2 and the remaining rays are order 1. Such a configuration is depicted in Fig. 22.

The top case of the multiplicative type Painlevé equations of [47] is one that has a symmetry group of type

$$W\big(E_8^{(1)}\big) = \langle s_0, \ldots, s_8 \rangle.$$

A presentation may be derived from the groups corresponding Dynkin diagram, which is shown below:



There are no Dynkin diagram automorphisms. We may specify the elemtents in terms of $\sigma_{i,j}$ as $s_0 = \sigma_{0,3}$, $s_1 = \sigma_{4,5}$, $s_2 = \sigma_{1,2}$, $s_4 = \sigma_{6,7}$, $s_5 = \sigma_{7,8}$,$s_6 = \sigma_{8,9}$, $s_7 = \sigma_{9,10}$ and $s_8 = \sigma_{10,11}$. The nontrivial actions are given by

$$
\begin{aligned}
&s_0\colon\ X \to X - B_0, \qquad s_2\colon\ Y \to Y + B_2,\\
&s_3\colon\ X \to X + \max(B_3, B_3 + X, Y) - \max(0, X, Y),\\
&s_3\colon\ Y \to Y - B_3 + \max(0, B_3 + X, Y) - \max(0, X, Y).
\end{aligned}
$$

By tracing around the figure, we find that

$$Q = 3B_0 + 2B_1 + 4B_2 + 6B_3 + 5B_4 + 4B_5 + 3B_6 + 2B_7 + B_8.$$

In the autonomous limit, this becomes a foliation of tropical sextic curves, specified by the level sets of

$$H(X, Y) = \max\{iX + jY + c_{i,j} \,|\, 0 \le i, 0 \le j, i + j \le 6\} - 2X - 3Y,$$

where

$$
\begin{aligned}
&c_{0,0} = 2\lambda_3, \qquad c_{0,2} = 2\lambda_2, \qquad c_{0,4} = 2\lambda_1,\\
&c_{1,1} = \max(2\kappa_2 + \mu_5, \kappa_1 - \kappa_2 + \lambda_2 + \lambda_3),\\
&c_{1,2} = \max(\kappa_1 - \kappa_2 + 2\lambda_2, 2\kappa_2 + \mu_5 + \lambda_2 - \lambda_3, \mu_1 + \lambda_3),\\
&c_{1,3} = \max(\mu_1 + \lambda_2, \kappa_1 - \kappa_2 + \lambda_1 + \lambda_2, 2\kappa_2 + \mu_5 + \lambda_1 - \lambda_3),\\
&c_{1,4} = \max(\mu_1 + \lambda_1, \kappa_1 - \kappa_2 + \lambda_2, 2\kappa_2 + \mu_5 - \lambda_3), \qquad c_{1,5} = \mu_1,\\
&c_{2,1} = \max(\kappa_1 + \kappa_2 + \mu_5, 2\kappa_1 - 2\kappa_2 + \lambda_2 + \lambda_3),\\
&c_{2,2} = \max(\kappa_2 + \mu_4, 2\lambda_2 - \kappa_2, \kappa_1 + \kappa_2 + \mu_5 + \lambda_2 - \lambda_3, \kappa_1 - \kappa_2 + \mu_1 + \lambda_3,\\
&\qquad\qquad 2\kappa_1 - 2\kappa_2 + \lambda_1 + \lambda_3),\\
&c_{2,4} = \mu_2, \qquad c_{3,0} = 3\kappa_1 - 3\kappa_2 + 2\lambda_3, \qquad c_{3,1} = \max(2\kappa_1 + \mu_5, \kappa_1 - 2\kappa_2 + \lambda_2 + \lambda_3),\\
&c_{3,2} = \max(\kappa_1 + \mu_4, \kappa_2 + \mu_5 + \lambda_2 - \lambda_3, -\kappa_2 + \mu_1 + \lambda_3, \kappa_1 - 2\kappa_2 + \lambda_1 + \lambda_3),\\
&c_{3,3} = \mu_3, \qquad c_{4,1} = \max(\kappa_1 + \mu_5, -2\kappa_2 + \lambda_2 + \lambda_3),\\
&c_{4,2} = \mu_4, \qquad c_{5,1} = \mu_5, \qquad c_{6,0} = \mu_6, \qquad c_{0,1} = c_{0,3} = c_{2,3} = -\infty,\\
&\max(0, X + \kappa_1, 2X + \kappa_2) = \max(0, X) + \max(0, X + B_0),\\
&\max(0, X + \lambda_1, 2X + \lambda_2, 3X + \lambda_3) = \max(0, X) + \max(0, X - B_2)\\
&\qquad + \max(0, X - B_1 - B_2),\\
&\max(0, X + \mu_1, \ldots, 6X + \mu_6) = \max(0, X + B_3)\\
&\qquad + \max(0, X + B_3 + B_4) + \cdots + \max(0, X + B_3 + B_4 + \cdots + B_8).
\end{aligned}
$$

The translation is the composition

$$
\begin{aligned}
T = {} & s_3 \circ s_2 \circ s_4 \circ s_3 \circ s_1 \circ s_2 \circ s_5 \circ s_4 \circ s_3 \circ s_6 \circ s_5 \circ s_4 \circ s_0 \circ s_3 \circ s_2 \circ s_1\\
& \circ s_7 \circ s_6 \circ s_5 \circ s_4 \circ s_3 \circ s_2 \circ s_8 \circ s_7 \circ s_6 \circ s_5 \circ s_4 \circ s_3 \circ s_0 \circ s_3 \circ s_4\\
& \circ s_5 \circ s_6 \circ s_7 \circ s_8 \circ s_2 \circ s_3 \circ s_4 \circ s_5 \circ s_6 \circ s_7 \circ s_1 \circ s_2 \circ s_3 \circ s_0 \circ s_4\\
& \circ s_5 \circ s_6 \circ s_3 \circ s_4 \circ s_5 \circ s_2 \circ s_1 \circ s_3 \circ s_4 \circ s_2 \circ s_3 \circ s_0.
\end{aligned}
$$

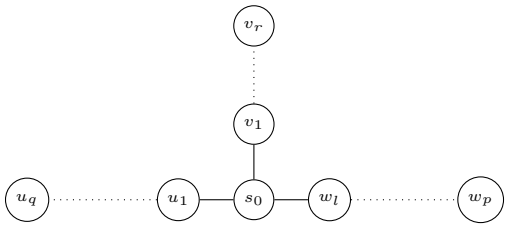


Figure 23. A Dynkin diagram of type $T_{p,q,r}$.

Once again, the evolution is too complicated in its tropical form to give here. However, the geometric interpretation is that the evolution is defined as

$$T(P) + T(L_i) = P + L_j, \tag{5.5}$$

where the addition is with respect to the group law on a tropical sextic genus one curve.

6 Discussion of dodecagons, triskaidecagons and higher

We wish to breifly discuss some of the difficulties extending the above arguments to more than eleven sides. We have two constructions that we believed were related; tropical maps of the plane arising from polygons with greater than 11 sides and tropical birational representations of the Weyl group $W(T_{p,q,r})$ constructed in [54], whose Dynkin diagram is given in Fig. 23.

Each one of the polygons we have considered so far arise from tropical genus one curves. If we go to a higher number of sides, a simple combinatorial argument based on (3.7) shows us that the higher sided polygons must come from higher genus cases. The simplest example is the autonomous system defined on a pencil of tropic quartics such that there are four distinct rays of order one in each direction. Suppose we parameterize these by

$$\begin{aligned}
&L_1\colon\ X = 0, && L_7\colon\ Y + B_7 + B_8 = 0,\\
&L_2\colon\ X - B_0 = 0, && L_8\colon\ Y + B_7 + B_8 + B_9 = 0,\\
&L_3\colon\ X - B_0 - B_1 = 0, && L_9\colon\ Y - X + B_3 = 0,\\
&L_4\colon\ X - B_0 - B_1 - B_2 = 0, && L_{10}\colon\ Y - X + B_3 + B_4 = 0,\\
&L_5\colon\ Y = 0, && L_{11}\colon\ Y - X + B_3 + B_4 + B_5 = 0,\\
&L_6\colon\ Y + B_7 = 0, && L_{12}\colon\ Y - X + B_3 + B_4 + B_5 + B_6 = 0,
\end{aligned}$$

as labelled in Fig. 24.

The diagram in Fig. 24 has been obtained by following a path in which the rays have been fixed, and follow the level curves of a biquartic invariant where three of the parameters, the coefficients of $X+Y$, $2X+Y$ and $X+2Y$, have been set to $-\infty$. Tracing around the diagram, we find that Q is given by

$$Q = 3B_0 + 2B_1 + B_2 + 4B_3 + 3B_4 + 2B_5 + B_6 + 3B_7 + 2B_8 + B_9.$$

Define a translation, T, by letting $T(L_i)$ move to a point that defines a pencil of closed polygons. For any point P, we have a unique closed curve, C, intersecting with P. The evolution defined by (5.3), (5.4) and (5.5) were in terms of a group law on genus one curves, however, these resulting closed curves in this more general setting are no longer of genus one, hence, describing the group structure on such curves is not so straightforward.

To obtain a higher number of sides (with the constraint that all rays of the same form are of the same order), we may realize 13-sided polygons as specializations of tropical curves of degree

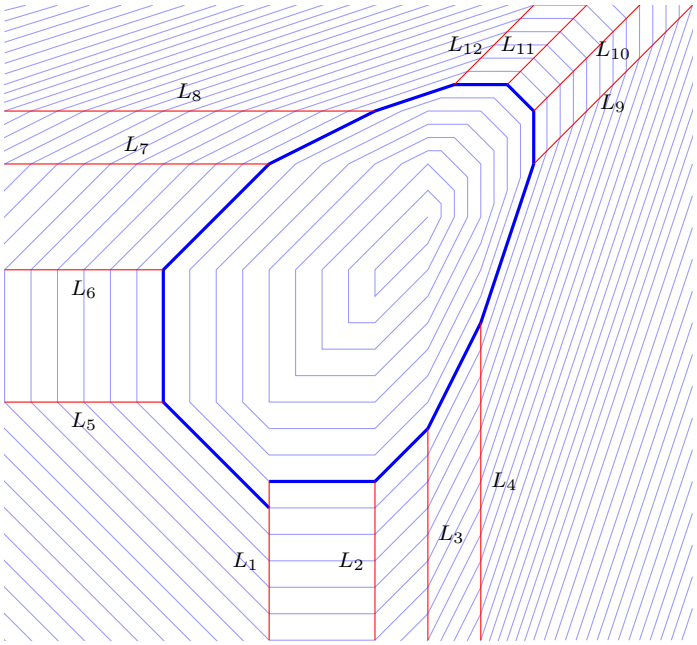


Figure 24. A model for the dodecagon.

twelve and 14-sided polygons as specializations of tropical curves of degree six. A rudimentary search reveals n-agons for all n up to 30 sides.

The problem is that in the autonomous limit, the naive extension to $W(T_{4,4,4})$ using canonical permutations and an analogue s_3 in the $E_8^{(1)}$ case does not preserve all the required quartic plane curves in the pencil constructed. The action of this generator generally gives a curve of degree five, hence, it is not s_3 invariant. It seems likely that this fails to preserve all the required degenerate curves when the closed piecewise linear curve become small. It seems that the dynamics we describe may have an interpretation in terms of the addition on some tropical hyper-elliptic curve, for example [11] where certain tropical dynamics was studied by using the tropical addition formulae on the spectral curve of hyper-elliptic type.

7 Conclusion

What has been presented is a way of naturally obtaining a group of transformations that preserve the structure of a spiral diagram. It is possible to extend this to cases that do not arise as ultradiscrete Painlevé equations, however the invariants seem more elusive. The autonomous limits do not necessarily result in foliations of genus one curves. Where the role of the addition law on cubic plane curves in the Painlevé equations and QRT maps is central [16], perhaps similar integrable systems could be based on the addition laws for hyperelliptic curves, which are in general, much more complicated [4, 11].

Another possible direction is to explore the tropical Cremona transformations more thoroughly. Interesting tropical versions of del Pezzo surfaces have emerged with $W(E_6)$ and $W(E_7)$ symmetry during the write-up of this paper [44]. A homological approach that follows [7, 24, 27, 28] more closely would also be of interest.

Acknowledgements

Christopher M. Ormerod would like to acknowledge Eric Rains for his helpful discussions. Y. Yamada is supported by JSPS KAKENHI Grant Number 26287018.

References

[1] Abramovich D., Karu K., Matsuki K., Włodarczyk J., Torification and factorization of birational maps, *J. Amer. Math. Soc.* **15** (2002), 531–572, math.AG/9904135.

[2] Bellon M.P., Viallet C.M., Algebraic entropy, *Comm. Math. Phys.* **204** (1999), 425–437, chao-dyn/9805006.

[3] Bieri R., Groves J.R.J., The geometry of the set of characters induced by valuations, *J. Reine Angew. Math.* **347** (1984), 168–195.

[4] Cohen H., Frey G., Avanzi R., Doche C., Lange T., Nguyen K., Vercauteren F. (Editors), Handbook of elliptic and hyperelliptic curve cryptography, *Discrete Mathematics and Its Applications*, Chapman & Hall/CRC, Boca Raton, FL, 2006.

[5] Dehli Vigeland M., The group law on a tropical elliptic curve, *Math. Scand.* **104** (2009), 188–204, math.AG/0411485.

[6] Dolgachev I.V., Iskovskikh V.A., Finite subgroups of the plane Cremona group, in Algebra, Arithmetic, and Geometry: in Honor of Yu.I. Manin, Vol. I, *Progr. Math.*, Vol. 269, Birkhäuser Boston, Inc., Boston, MA, 2009, 443–548, math.AG/0610595.

[7] du Val P., On the Kantor group of a set of points in a plane, *Proc. London Math. Soc.* **S2-42** (1937), 18–51.

[8] Duistermaat J.J., Discrete integrable systems. QRT maps and elliptic surfaces, *Springer Monographs in Mathematics*, Springer, New York, 2010.

[9] Gathmann A., Tropical algebraic geometry, *Jahresber. Deutsch. Math.-Verein.* **108** (2006), 3–32, math.AG/0601322.

[10] Hudson H.P., Cremona transformations in plane and space, Cambridge University Press, Cambridge, 1927.

[11] Inoue R., Takenawa T., Tropical spectral curves and integrable cellular automata, *Int. Math. Res. Not.* **2008** (2008), Art ID. rnn019, 27 pages, arXiv:0704.2471.

[12] Isojima S., Grammaticos B., Ramani A., Satsuma J., Ultradiscretization without positivity, *J. Phys. A: Math. Gen.* **39** (2006), 3663–3672.

[13] Jimbo M., Sakai H., A q-analog of the sixth Painlevé equation, *Lett. Math. Phys.* **38** (1996), 145–154, arXiv:chao-dyn/9507010.

[14] Joshi N., Lafortune S., Integrable ultra-discrete equations and singularity analysis, *Nonlinearity* **19** (2006), 1295–1312.

[15] Joshi N., Nijhoff F.W., Ormerod C., Lax pairs for ultra-discrete Painlevé cellular automata, *J. Phys. A: Math. Gen.* **37** (2004), L559–L565.

[16] Kajiwara K., Masuda T., Noumi M., Ohta Y., Yamada Y., ${}_{10}E_9$ solution to the elliptic Painlevé equation, *J. Phys. A: Math. Gen.* **36** (2003), L263–L272, nlin.SI/0303032.

[17] Kajiwara K., Masuda T., Noumi M., Ohta Y., Yamada Y., Point configurations, Cremona transformations and the elliptic difference Painlevé equation, in Théories asymptotiques et équations de Painlevé, *Sémin. Congr.*, Vol. 14, Soc. Math. France, Paris, 2006, 169–198.

[18] Kajiwara K., Masuda T., Noumi M., Yamada Y., Tropical affine Weyl group representation of type $E_n^{(1)}$, 2004.

[19] Kajiwara K., Noumi M., Yamada Y., A study on the fourth q-Painlevé equation, *J. Phys. A: Math. Gen.* **34** (2001), 8563–8581, nlin.SI/0012063.

[20] Kajiwara K., Noumi M., Yamada Y., Discrete dynamical systems with $W(A_{m-1}^{(1)} \times A_{n-1}^{(1)})$ symmetry, *Lett. Math. Phys.* **60** (2002), 211–219, nlin.SI/0106029.

[21] Kanki M., Mada J., Tokihiro T., Conserved quantities and generalized solutions of the ultradiscrete KdV equation, *J. Phys. A: Math. Theor.* **44** (2011), 145202, 13 pages, arXiv:1012.4061.

[22] Kasman A., Lafortune S., When is negativity not a problem for the ultradiscrete limit?, *J. Math. Phys.* **47** (2006), 103510, 16 pages, nlin.SI/0609034.

[23] Kondo K., Ultradiscrete sine-Gordon equation over symmetrized max-plus algebra, and noncommutative discrete and ultradiscrete sine-Gordon equations, *SIGMA* **9** (2013), 068, 39 pages, arXiv:1311.2675.

[24] Looijenga E., Rational surfaces with an anticanonical cycle, *Ann. of Math.* **114** (1981), 267–322.

[25] Markwig T., A field of generalised Puiseux series for tropical geometry, *Rend. Semin. Mat. Univ. Politec. Torino* **68** (2010), 79–92, arXiv:0709.3784.

[26] Murata M., Exact solutions with two parameters for an ultradiscrete Painlevé equation of type $A_6^{(1)}$, *SIGMA* **7** (2011), 059, 15 pages, arXiv:1106.3384.

[27] Nagata M., On rational surfaces. I. Irreducible curves of arithmetic genus 0 or 1, *Mem. Coll. Sci. Univ. Kyoto Ser. A Math.* **32** (1960), 351–370.

[28] Nagata M., On rational surfaces. II, *Mem. Coll. Sci. Univ. Kyoto Ser. A Math.* **33** (1960/1961), 271–293.

[29] Nobe A., Ultradiscrete QRT maps and tropical elliptic curves, *J. Phys. A: Math. Theor.* **41** (2008), 125205, 12 pages.

[30] Nöther M., Ueber die auf Ebenen eindeutig abbildbaren algebraischen Flächen, *Gött. Nachr.* (1870), 1–6.

[31] Noumi M., Yamada Y., Affine Weyl groups, discrete dynamical systems and Painlevé equations, *Comm. Math. Phys.* **199** (1998), 281–295, math.AG/9804132.

[32] Ochiai T., Nacher J.C., Inversible max-plus algebras and integrable systems, *J. Math. Phys.* **46** (2005), 063507, 17 pages, nlin.SI/0405067.

[33] Okamoto K., Sur les feuilletages associés aux équations du second ordre à points critiques fixes de P. Painlevé. Espaces des conditions initiales, *Japan. J. Math. (N.S.)* **5** (1979), 1–79.

[34] Ormerod C.M., Hypergeometric solutions to an ultradiscrete Painlevé equation, *J. Nonlinear Math. Phys.* **17** (2010), 87–102, nlin.SI/0610048.

[35] Ormerod C.M., Reductions of lattice mKdV to q-P_{VI}, *Phys. Lett. A* **376** (2012), 2855–2859, arXiv:1112.2419.

[36] Ormerod C.M., Tropical geometric interpretation of ultradiscrete singularity confinement, *J. Phys. A: Math. Theor.* **46** (2013), 305204, 15 pages, arXiv:0802.1959.

[37] Papageorgiou V.G., Nijhoff F.W., Grammaticos B., Ramani A., Isomonodromic deformation problems for discrete analogues of Painlevé equations, *Phys. Lett. A* **164** (1992), 57–64.

[38] Pin J.E., Tropical semirings, in Idempotency (Bristol, 1994), *Publ. Newton Inst.*, Vol. 11, Cambridge University Press, Cambridge, 1998, 50–69.

[39] Quispel G.R.W., Capel H.W., Scully J., Piecewise-linear soliton equations and piecewise-linear integrable maps, *J. Phys. A: Math. Gen.* **34** (2001), 2491–2503.

[40] Quispel G.R.W., Roberts J.A.G., Thompson C.J., Integrable mappings and soliton equations, *Phys. Lett. A* **126** (1988), 419–421.

[41] Quispel G.R.W., Roberts J.A.G., Thompson C.J., Integrable mappings and soliton equations. II, *Phys. D* **34** (1989), 183–192.

[42] Ramani A., Grammaticos B., Hietarinta J., Discrete versions of the Painlevé equations, *Phys. Rev. Lett.* **67** (1991), 1829–1832.

[43] Ramani A., Takahashi D., Grammaticos B., Ohta Y., The ultimate discretisation of the Painlevé equations, *Phys. D* **114** (1998), 185–196.

[44] Ren Q., Shaw K., Sturmfels B., Tropicalization of del Pezzo surfaces, arXiv:1402.5651.

[45] Richter-Gebert J., Sturmfels B., Theobald T., First steps in tropical geometry, in Idempotent mathematics and mathematical physics, *Contemp. Math.*, Vol. 377, Amer. Math. Soc., Providence, RI, 2005, 289–317, math.AG/0306366.

[46] Rojas O., From discrete integrable systems to cellular automata, Ph.D. Thesis, La Trobe University, Australia, 2009.

[47] Sakai H., Rational surfaces associated with affine root systems and geometry of the Painlevé equations, *Comm. Math. Phys.* **220** (2001), 165–229.

[48] Scully J., An exploration of integrable two-dimensional maps, Honours Thesis Mathematics Department, La Trobe University, Australia, 1999.

[49] Takahashi D., Matsukidaira J., Box and ball system with a carrier and ultradiscrete modified KdV equation, *J. Phys. A: Math. Gen.* **30** (1997), L733–L739.

[50] Takahashi D., Tokihiro T., Grammaticos B., Ohta Y., Ramani A., Constructing solutions to the ultradiscrete Painlevé equations, *J. Phys. A: Math. Gen.* **30** (1997), 7953–7966.

[51] Tokihiro T., Takahashi D., Matsukidaira J., Box and ball system as a realization of ultradiscrete nonautonomous KP equation, *J. Phys. A: Math. Gen.* **33** (2000), 607–619.

[52] Tokihiro T., Takahashi D., Matsukidaira J., Satsuma J., From soliton equations to integrable cellular automata through a limiting procedure, *Phys. Rev. Lett.* **76** (1996), 3247–3250.

[53] Tsuda T., Integrable mappings via rational elliptic surfaces, *J. Phys. A: Math. Gen.* **37** (2004), 2721–2730.

[54] Tsuda T., Tropical Weyl group action via point configurations and τ-functions of the q-Painlevé equations, *Lett. Math. Phys.* **77** (2006), 21–30.